Wave-Powered Pulse Flow Reverse Osmosis Desalination System

Marine Energy Collegiate Competition 2024
Purdue University Team

PEARL JAAMS

David Warsinger	Faculty Advisor	david.warsinger@gmail.com
Maia Catterall	Mechanical Engineering Undergrad Researcher	mcatter@purdue.edu
Jeff Huang	Mechanical Engineering Undergrad Researcher	huan1543@purdue.edu
Abby Zahm	Mechanical Engineering Undergrad Researcher	ajzahm@purdue.edu
Sofia Loucks	Mechanical Engineering Undergrad Researcher	louckss@purdue.edu
Akash Mattupalli	Mechanical Engineering Undergrad Researcher	amattupa@purdue.edu
Ali Naderi Beni	Mechanical Engineering PhD Candidate	anaderib@purdue.edu
Sultan Alnajdi	Mechanical Engineering PhD Candidate	salnajdi@purdue.edu
Oscar Botia	Mechanical Engineering Undergrad Researcher	obotiasi@purdue.edu
Nikitha Sam	Mechanical Engineering Undergrad Researcher	nsam@purdue.edu
Janoah Darrow	Mechanical Engineering Undergrad Researcher	darrowj@purdue.edu
Joel Aboderin	Mechanical Engineering PhD Candidate	jaboderi@purdue.edu

Report	Word Count
Business Report	4637
Technical Report	5115
Build and Test Report	4908

Table of Contents

1 Executive Summary

With the onset of climate change and global warming, coastal communities, such as those in Puerto Rico, are especially vulnerable to natural disasters. Hurricanes have made maintaining access to clean water difficult with unreliable sources of power. Given the established industry standard of externally powered desalination facilities, or costly devices with internal electronics, it is important to develop a passive, purely mechanical device capable of filtering water from renewable tidal wave energy, to meet remote, coastal communities' water insecurity issues as a disaster relief measure.

Tackling this water insecurity sustainably is multi-faceted, as it involves stakeholders like Puerto Rico, the Department of Energy, and Warsinger Water Lab with their varied involvements in the design and deployment process of a Pulse Flow Reverse Osmosis (PFRO) solution. The needs of disaster-stricken communities in Puerto Rico are central to the team's design, and the proposed solution will also require minimal maintenance, as accounted for by the low risks of membrane fouling. Thus, the team created a PFRO system consisting of a piston, membrane, and a "brine-blocking" mechanism to selectively allow permeate or brine production. The PFRO system, which would be enclosed within a buoy and anchored to the sea floor, would be powered by a wave energy converter (WEC).

The decision to pursue PFRO for the proposed solution was based on market research on existing reverse osmosis techniques, such as continuous and batch reverse osmosis, and the evaluation of the marine energy market. The analysis states that the marine energy market is estimated to have a compound annual growth rate of 21.20% (Precedence Research), with positive push for green energy from the government, the large applicability of the product, and the unique values the product offers that fills the gap in the market for passive RO systems.

The device design began with a kinematic analysis of a purely mechanical crank-arm mechanism. With the values for net heave force from an irregular wave pattern, and a complex WEC design consisting of a rack and pinion, ratchet and pawl, and gearbox the team began designing a purely mechanical PFRO system. Due to the limitations of the testing facilities, the team decided to simulate the oscillating motion of the crank-arm subassembly with a pump and two 3/2 valves to deliver pressurized water to both chambers in the piston cylinder, resulting in the piston's actuation. Thus, the energy requirements of the system would be accurately estimated.

After completing the build of the PFRO system, a series of tests were conducted to validate the PFRO process. Both regular and irregular waves were tested to ensure the PFRO system performed under ideal and non ideal conditions. The results include a peak pressure of 890 psi, peak permeate flow rate of 0.439 L/min, recovery ratio of 29%, and power consumption of 37.1

kWh/m^3 of permeate. These findings provide compelling evidence regarding the effectiveness of the device, confirming that the PFRO process is successfully validated.

2 Business Plan

2.1 Concept Overview

The proposed design is a ***Wave-Powered Pulse Flow Reverse Osmosis Desalination System.*** Utilizing the rising and falling energy of ocean waves, this system is able to harness renewable ocean energy and convert seawater into clean, drinkable water employing the novel desalination technique of pulse flow reverse osmosis (PFRO). The design will be purely mechanical. Therefore, the system will be able to desalinate water without any electrical components or additional power sources. This greatly reduces maintenance requirements as well as increases robustness and simplicity.

The team's key vision is to provide a semi-permanent source of fresh, potable water that will bridge the gap between initial disaster relief aid and the repair of long-term infrastructure in coastal communities. After negotiating a contract with the U.S. government, specifically the Federal Emergency Management Agency (FEMA), the team will deploy an all-in-one device, as described above, to provide clean water to disaster-stricken communities. The water will then be sold to local governments at a price marginally above municipal water supplies, allowing the organization to recoup costs and generate profit. The devices could then be sold to local governments after the initial contract period to supplement their water production and relieve shipping and energy burdens. However, the current plan is to rotate devices out of communities as necessary.

By implementing this device in areas without sufficient fresh water infrastructure, the team can provide tremendous social value as desalinating drinking water will significantly accelerate the recovery process for these coastal communities.

2.2 Stakeholders

The primary stakeholders are the residents of disaster-stricken coastal communities. As end users of the product, the device must be chiefly geared to meet their requirements. To achieve this, the team has identified the community of San Juan, Puerto Rico as one such community in the United States representative of the larger market. Therefore, it became the main location for gathering data for the planned system and the initial solution design was developed based on its parameters.

The next stakeholder is Dr. David Warsinger of Purdue University's Warsinger Water Lab. An expert in the reverse osmosis industry, the Purdue MECC team is working closely with Dr. Warsinger's research team to develop and validate a novel desalination technique: Pulse Flow

Reverse Osmosis. Any patent or licensure obtained for this design would impact the lab's funding, so it was paramount that their resources were correctly allocated.

The last stakeholder is the United States Department of Energy (DOE). Through sponsoring the Marine Energy Collegiate Competition, the DOE is pushing the development of unique solutions to challenges faced by the marine energy industry.

2.2.1 Discussion with Industry Professionals and End Users

In order to better understand the needs of the end users, the team conducted a series of interviews with 3 industry professionals: Dr. David Warsinger, Dr. José Garcia-Bravo, and Quantum Wei.

Dr. David Warsinger - Assistant Professor of Mechanical Engineering at Purdue University
Through a series of conversations with Dr. Warsinger, the team gained insight on the intricacies of reverse osmosis systems and their common challenges. With years of desalination research and his foundation of the Warsinger Water Labs at Purdue, he condensed relevant and complex industry information on the novelty and applications of different desalination techniques. As a key stakeholder, Dr. Warsinger guided the team in recognizing the novelty of the PFRO design and ensured its uniqueness compared to other desalination techniques, such as batch and continuous RO. This allowed the team to pursue the validation of a new PFRO design while also being realistic about its usefulness.

Dr. José Garcia-Bravo - Associate Professor of Engineering Technology at Purdue University
In the team's discussions with Dr. Garcia, who has been nationally recognized and awarded for his research in applied fluid power, he emphasized the importance of operational safety. This applies to both the end users as well as the undergraduate researchers during the prototype building phase. With pressures reaching up to 890 psi, safety must be the top priority. Dr. Garcia highlights that leaks pose the greatest concern. Not only can leaks prevent the system from reaching the desired pressure but, from a safety perspective, these high pressure leaks can easily penetrate skin if mishandled. Therefore, he stresses that the system must not be touched while in operation, and any modifications performed must be done when the system is switched off and completely depressurized.

Quantum Wei - CEO of Harmony Desalting
Harmony Desalting, a company started by Quantum, has the mission statement of providing a more affordable and sustainable approach to desalination through using batch reverse osmosis. In the interview, the primary concern Quantum brought up for the end users is testing. He is currently testing a novel component in desalination that involves a pressurized bladder for his own company. He must demonstrate to his investors that his design can not only handle certain pressures but also last for 10 years. Since it is unrealistic to run a test for a period of 10 years, Quantum devised an approach to model the feasibility of the design by putting the device under

pressures exceeding normal operation conditions and significantly reducing cycle time. Subjecting the bladder to these extreme conditions proves that the bladder can ensure the projected lifespan under normal conditions. Based on his testing experience, Quantum recommends testing the system under conditions higher than what a typical end user would experience. This insight provides valuable guidance for the team's testing approach following the build process.

Through these three interviews, the team has received guidance that has significantly strengthened the direction of the design process. Considering factors like novelty, safety, and testing, the design is more tailored to meeting the needs of end users.

2.3 Market Opportunity

2.3.1 Competition

Analyzing the current competition, Oneka Technologies' wave-powered desalination system and various emergency filtration systems meet the same market needs for clean drinking water. However, Oneka Technologies uses conventional reverse osmosis while Pearl JAAMS's device uses pulse flow reverse osmosis (Patent No: US 11,130,097 B2). Harnessing wave energy, a crank arm system, and a piston, PFRO outputs higher efficiency and has a lower risk of biofouling compared to conventional reverse osmosis. According to Oneka's website their smallest model, IceCube, produces 256 gallons/day, their middle model, Iceberg, makes 13k gallons/day, and the largest model, Glacier, makes 132k gallons/day (Oneka). These can be seen below in Figure 2.1. For perspective, the average American uses about 82 gallons/day according to the U.S Environment Protection Agency, so the IceCube produces about 3x the amount the average American uses (Environmental Protection Agency).

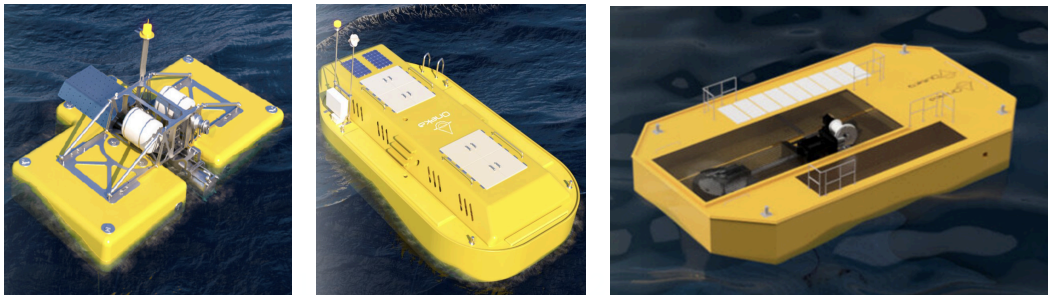

Figure 2.1: Oneka Technologies Wave Powered Desalination Systems (IceCube, Iceberg, Glacier)

Another product on the market is made by Resolute Marine. This design is on a larger scale and a more permanent system, where a pendulum-like object is installed into a shallow part of the ocean and can flow back and forth with the waves moving around it. The energy generated from this pendulum mechanism powers a reverse osmosis system on land and the clean water is then stored on land. Finally, the last product is the gravity-powered emergency water filtration system by Outback Water. This system only filters about 24 gallons/day of water and is for mainly

freshwater as it only filters out contaminants such as dirt or algae (Outback). These products can be seen in Figure 2.2 below.

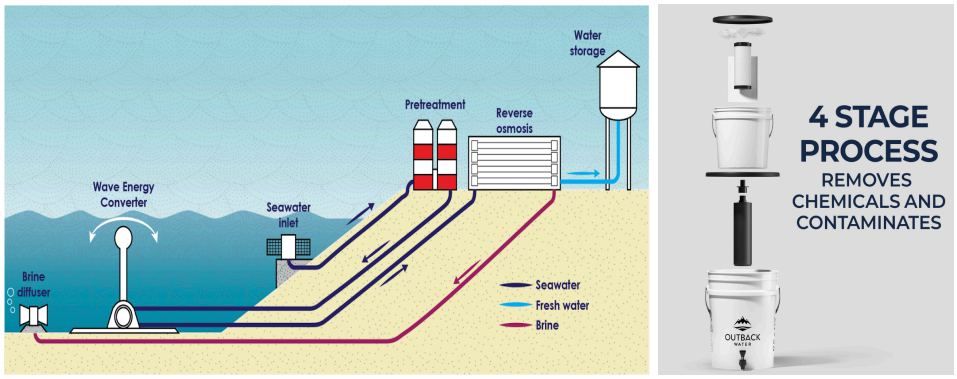

Figure 2.2: Resolute Marine & Outback Water

The last product on the market the team analyzed is Outback Water's Gravity Powered Filtration System, which can only filter from freshwater sources like rivers and lakes. In contrast, PFRO can purify both sea and freshwater, making it more versatile than current emergency filtration products.

Pearl JAAMS also looked into any current patents to prevent any interference with them. The most relevant current patent was Oneka Technologies' who patented their process and method for water desalination using continuous reverse osmosis and hyperfiltration. Another applicable patent was developed by King Abdullah University of Science and Technology, who patented their process for inhibiting membrane biofouling. Both of these patents can be seen in Figure 2.3 below.

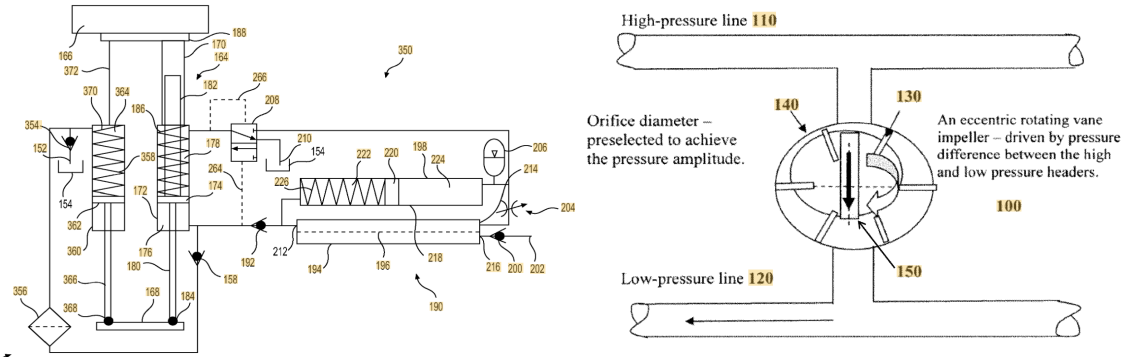

Figure 2.3: (Left to Right) Diagram from Oneka Technologies Patent & King Abdullah University of Science and Technology (KAUST)

Lastly, Pearl JAAMS looked at alternative solutions on the market to get inspiration and ensure there were no other alternatives they wanted to pursue. The first alternative is electrodialysis which utilizes positively and negatively charged ions to filter water (Lenntech) and the second

alternative is desalination via sunlight, where the sun evaporates salt water in a transparent tank and the clean water condenses at the top and is collected. Diagrams of these alternatives can be seen in Figure 2.4 below.

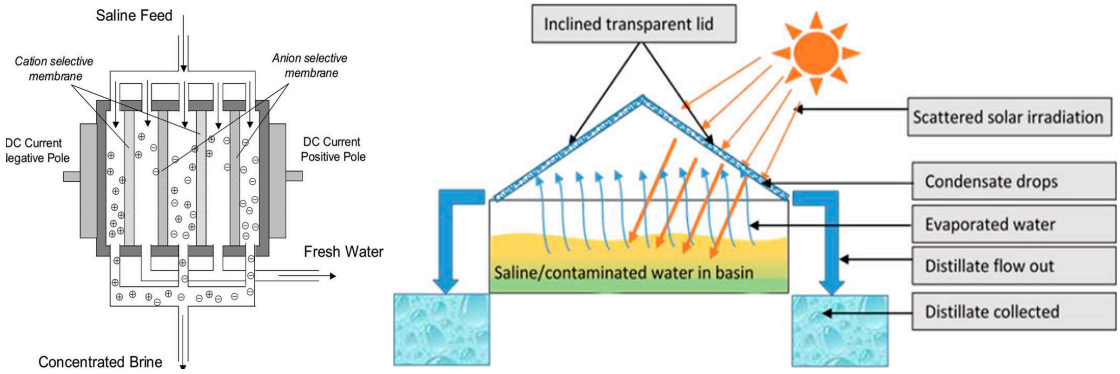

Figure 2.4: Electrodialysis and Desalination via Sunlight

2.3.2 Blue Market Economy

In addition to current products, patents, and relevant systems, the marine energy market was also analyzed. This market was found to be favorable due to the large market growth for the future, and the team is confident that their project could capitalize on the opportunity. According to Precedence research, "The global marine energy market size was estimated at USD 914.2 million in 2022 and is anticipated to reach around USD 6,226.78 million by 2032." The marine energy industry is predicted to boom and grow immensely by 6.8x its current worth, which makes it a very profitable industry to invest in. Through this comprehensive analysis, the team determined that there was an economic and societal niche for a small-to-moderate sized PFRO system that function purely passively in order to reduce maintenance requirements.

2.3.3 PFRO Value Overview

The wave-powered pulse flow reverse osmosis desalination system is designed to meet the pressing needs of disaster-stricken coastal communities. Following natural disasters such as hurricanes, infrastructure damage makes it extremely challenging for communities to have access to essential resources such as potable water. For example, according to the Washington Post, following the devastation caused by Hurricane Maria, Puerto Rico suffered from a severe shortage of fresh water due to the complete collapse of the power grid. This rendered water treatment facilities inoperable and despite weeks following the disaster, Puerto Ricans are still in dire need of water. 6 months after Hurricane Maria a third of the population of San Juan (300,000) did not have access to safe drinkable water and some resorted to consuming unsafe sources, leading to bacterial infections (Panditharatne).

Pearl JAAMS's design will aim to immediately address this issue through desalinating seawater using only wave energy. By deploying the device along the coast, desalination can begin swiftly,

providing immediate relief to these affected communities. This not only alleviates the burden of getting access to clean water but also enables these communities to focus their efforts on other pressing issues.

Furthermore, with global warming on the rise, the issue of natural disasters will only become more severe and frequent. Consequently, the demand for solutions like the team's will only grow, expanding the market for such technologies. The map below demonstrates areas that experience water scarcity.

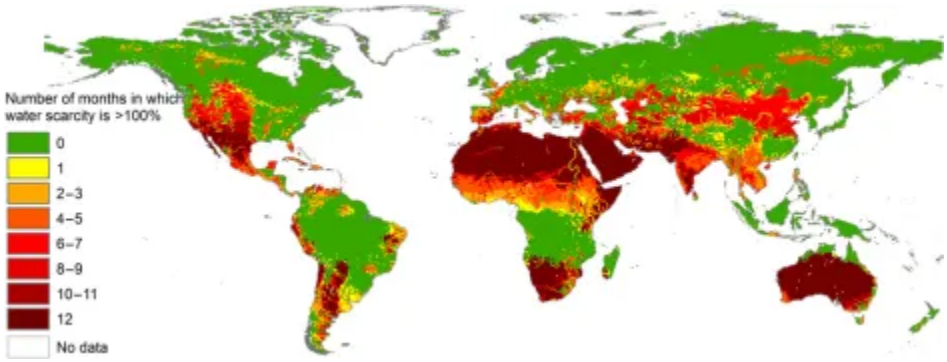

Figure 2.5: Map of Regions of Water Scarcity (Carylsue, 2016)

The initial pricing for the PFRO system considers production and material costs, operational expenses, and the cost of bottled water. The cost of bottled water is included as Pearl JAAMS wants their product to be more cost efficient than transporting bottled water to the community. A rotational program is also implemented to move these systems once a disaster-stricken community is back on its feet to improve affordability for the target distributors. Table 2.1 displays a competitive analysis between PFRO and its competitors for various metrics.

The team also determined the perceived value of the product via market research and analyzing stakeholders' predicted budgets for relief to understand how much consumers would be willing to pay. Combining the initial pricing with consumers' perceived value assists in finding the right price point for both the producers and the consumers.The team believes that a PFRO system is the preferred choice for drinking water disaster relief efforts through the unique affordability and efficiency.

Table 2.1: Competitive Analysis

Product	Gallons of Permeate/day	Recovery Ratio	$/Gallon of Water
San Juan Water District	-	-	$0.0014

Bottled Water	-	-	$4.50
Outback	24	~100%	$8.33
Oneka	265	20-35%	-
Pearl JAAMS	380	29%	$0.02

2.4 Development and Operations

2.4.1 Technical Barriers

A key barrier the team will be faced with when expanding this project into a viable, long-term business is the manufacturing and tolerancing of both the rack and pinion and crank arm mechanisms. The unique gearbox specifications and high torque loads means that the parts will likely need to be manufactured using costly processes such as CNC-machining. To reduce these costs, the team should explore other contracted opportunities, perhaps with a casting manufacturer to reduce these costs.

Another risk factor with this project is the high pressures the system will occasionally produce. Key components can be protected from over-pressurization by utilizing a pressure relief valve that would siphon high-pressure flow from the system. However, this diversion of flow leads to a reduction in the feed flow that enters the system during the permeate phase, and thus, a reduction in the total permeate production rate. To circumvent this issue, the team should modify the pressure vessel used to have a higher rated pressure, and thus, a higher threshold can be set on the pressure relief valve. Alternatively, the team can investigate a solution where approximately half of the pressure relief stream is released to the surrounding ocean, and the other half is recirculated back to the intake port. With a combination of these changes, the team would mitigate the risks of failure from overpressurization, and risk of poor performance.

Additionally, the team would like to undertake additional longitudinal testing to ensure the product suffers no cyclic failure on key components such as the crank arm mechanism and buoy shell. However, no such test facilities are operational at Purdue University. Thus, the team would have to seek an outside partnership, perhaps with an additional university, to manufacture and test the full configuration. As of yet, the crank arm design is still in the modeling phase and has not been physically integrated with the full PFRO system. Longitudinal testing would mitigate the risk of unanticipated mechanical failure during end-user deployment.

2.4.2 Operations and Maintenance

Once the system is placed little maintenance is required, so community members aren’t required to learn extra skills or frequently check on the system. This is due to utilizing PFRO, because the separate permeate and flushing cycles increase the longevity of the filter membrane before it

needs to be changed. The membranes can be used for up to 2 years on one side and then flipped to the other for an additional 2 years.

Anticipated operations and maintenance checks are planned between rotations of the buoy device, so they can be fixed and/or cleaned before being placed to aid a different community. Membranes would be monitored, inspected, and flipped/replaced during the scheduled check between locations. Mechanical components would be verified for daily operations and lubed/replaced when needed. For emergency operations or maintenance, members of the emergency relief response organization will be trained and prepared to fix common issues.

To compare most gravity powered or basic filtration drinking water solutions require hourly maintenance to be refilled or cleaned out depending on the volume of water. For a typical fossil fuel driven desalination plant, maintenance and operation checks are more extensive and are required more frequently due to the scale. The membranes also need to be changed faster due to the volume of water being pushed through them every day. Lastly, for solar panels, maintenance checks are needed 2 to 4 times per year (Gerhardt), so they can be cleaned off to improve operational efficiency. This maintenance frequency is likely increased if the panels are used on or near sea water due to salt and marine life accumulating on the panels.

2.5 Financial and Benefits Analysis

After confirming the final design, the market potential, and the target customer group of San Juan, the team conducted a value proposition using a Present Worth analysis. Three key components were considered; costs, profits, and production sizing.

2.5.1 Assumptions

To accurately size the amount of units the team could ideally produce, the team used statistics about San Juan's population. The average resident in San Juan consumes 91.3 gallons of water per day (KPCC). Additionally, San Juan's total population is approximately 326,950 people as of 2020 (United States Census Bureau, 2024). Using these two statistics, the average annual water consumption of the city can be computed. As the intent of the project is as an emergency solution, the team used the goal of 5% of San Juan's annual water production, and the final design's estimated flow rate of 1 L/min to calculate the required number of devices. To fulfill the 5% goal, 3,923 devices would need to be operational. To confirm the feasibility of this estimation, the team then estimated the deployment area available along the north coast of the island. Using a north coast length of approximately 111 miles, and a device width of 5 ft, with 10 ft of spacing between each device, the maximum possible number of devices can be calculated - 39,072 (Mathews et. al, 2024). As this number does not account for the density of deployment, it can be seen as a conservative maximum estimate. Thus, the team's initial estimate of 3,923 devices is reasonable and was used in calculations moving forward.

2.5.2 Costs

The initial costs, composed of assembly labor, part purchase costs, and overhead, were estimated using the purchasing price, and an adjustment for the purchased volume. Labor costs, including assembly and monthly device maintenance, were assumed to be constant at a rate of $60/hr. The cost of manufacturing each device was calculated to be $5,870.59. For the crank arm mechanism, purchased parts were used to estimate costs, as it was difficult to quantify the total equipment or outsourcing that would be necessary. The team is confident that these industry standard parts provide an accurate estimate to create this mechanism. To yield a conservative estimate, the team also included the cost of shipping and device deployment in the initial investment costs. Shipping was assumed to be a flat rate of $500 per device with a deployment time of half an hour at the hourly labor rate of $60 (for skilled labor). Next, the team calculated annual costs, consisting of maintenance per device. Assuming 1 hour of maintenance per month, the annual maintenance cost per device was calculated to be $720 annually. Deploying and shipping all the devices was estimated to cost a net of $2,079,190.00.

2.5.3 Revenues

Next, the team estimated the main revenue stream - selling the water produced at a flat rate to the local government of San Juan. To determine a reasonable price, the team evaluated alternatives in the area. The price per CCF for municipal water in the city is $1.07 (San Juan Water District, 2024), while the price of bottled water is $1.79 per liter (Puerto Rico - bottled water - price, January 2024, 2024). Due to the urgent nature of water production post-disaster, the team decided that a reasonable price would be $0.02 per gallon, or about 10 times the cost of municipal water. This is to combat the high investment and rapid deployment costs the project would incur. However, this is still a 97% reduction in price when compared to the most common water relief tool - bottled water. The above analysis, when combined with the device flow rate, yielded a net annual revenue of $28,461.02 per device.

The above net investment costs, annual revenues, and annual maintenance costs were then used to calculate the net cash flow each year. In the first year of operation, the complete distribution of devices would yield a net cash flow of $108,828,021.71, with an investment cost of $25,109,509.77. Every second year, the filter membrane has to be replaced, which varies the cash flow to $107,815,079.06. The analysis was completed assuming a net useful life of 5 years of the device, due to their semi-permanent nature, and a conservative mean average rate of return (MARR) of 15%. This yielded a present net worth of $338,353,814.58. As this value is positive, the project is a sound investment. To better understand the real value of the project, the net worth was then adjusted for inflation of 3.4%, with a base year of 2024. The real value of this project is thus, $307,093,479.45 in the year 2024.

This analysis helped the team determine that expansion into this market has real potential to be profitable, and the spreadsheet created to conduct these calculations is modular to assess the project value throughout design phases. A subset of the sheets is shown below.

Table 2.1: Device Profit and Production Amount Calculations

Profit Calculation			**Sizing Criteria**		
San Juan Water Rate ($/gal) :	$0.00143		**Water Use (gallons/day):**	91.3	per resident
Number of Assembly:	3923		**Water Use (L/yr):**	41243727498	
Disaster Factor:	10.00		**gal/L**	3.78541	
Water Flow Rate (L/min):	1		**Total Water Use (L/day)**	112996513.7	
Min/year	525600		**Population of San Juan:**	326,950	
			Market Share:	5.0%	
Net Water Flow Rate (L/yr)	525600.0		**Needed Fluid Production (L/yr):**	2062186375	
Profit/Assembly($/yr):	$28,461.02		**Number of Devices Required:**	3923	
Total Annual Profit:	$111,652,581.71				

Table 2.2: Production Amount Validation

Puerto Rico Space Evaluation:				
Width of island	39	mi		
North shore coastline	111	mi		
Distance between each device	10	ft	0.001893939394	miles
Device Size	5	ft	0.000946969697	miles
Max Area per Device:	0.002840909091	mi		
Max Number of Devices:	39072			
Percentage of Max:	10.04%			
Number of Units:	3923			

Table 2.3: Component Costs

Component 1: Purchased Piston Assembly	
Description	SS Piston assembly of 1.2 L volume, Bore: 60 mm; Rod: 30 mm; Stroke 500 mm;
Vendor	JIT Industries
Retail Cost	$1,828.00
Units/yr.	3,923.00
Volumized % of retail	90%
Part Cost	$1,645.20
Overhead	8.5%
Component Cost	$1,785.04

Component 2: Purchased Membrane	
Description	DOW Filmtec SW30-2540,2.5" Diameter x 40" Length; 800 psi; 55 bar
Vendor	Big Brand Water Filter
Retail Cost	$264.42
Units/yr.	3,923.00
Volumized % of retail	90%
Part Cost	$237.98
Overhead	8.5%
Component Cost	$258.21

Component 3: Purchased Pilot-Operated Valve Assembly	
Description	GL STAINLESS STEEL INLINE PILOT OPERATED CHECK VALVE, SINGLE ACTING, 3/8" BSP PORTS
Vendor	FlowFit
Retail Cost	$427.89
Units/yr.	3,923.00
Volumized % of retail	90%
Part Cost	$385.10
Overhead	8.5%
Component Cost	$417.83

Component 4: Purchased Pressure Vessel	
Description	2.5" x 40" Fiberglass/FRP Seawater Membrane Housing Pressure Vessel
Vendor	WaterAnywhere
Retail Cost	$614.99

Component 5: Purchased Rubber Hosing	
Description	Rubber Hosing 1/4"
Vendor	Commercial Rubber & Equipment
Retail Cost	$2.34

Component 6: Purchased Check Valves	
Description	316 Stainless Steel Check Valve with Fluoroelastomer Piston
Vendor	McMaster-Carr
Retail Cost	$55.83

Units/yr.			**Units/yr.**	3,923.00		**Units/yr.**	15692
Volumized % of retail	95%		**Volumized % of retail**	90%		**Volumized % of retail**	70%
Part Cost	$584.24		**Part Cost**	$2.11		**Part Cost**	$39.08
Overhead	8.5%		**Overhead**	8.5%		**Overhead**	8.5%
Component Cost	$633.90		**Component Cost**	$2.29		**Component Cost**	$42.40
Component 7: Purchased T Connectors			**Component 8: Purchased Pressure Vessel Fittings**			**Component 9: Pressure Relief Valve**	
Description	High-Pressure 304 Stainless Steel Pipe Fitting, Tee Connector, 1/4 NPT Female		**Description**	1/4" Male NPT Hose		**Description**	Pressure Release valve: 0-1000psi
Vendor	McMaster-Carr		**Vendor**	Commercial Rubber and hosing		**Vendor**	McMaster-Carr
Retail Cost	$26.37		**Retail Cost**	$614.25		**Retail Cost**	$385.00
Units/yr.	7846		**Units/yr.**	11769		**Units/yr.**	3,923.00
Volumized % of retail	80%		**Volumized % of retail**	70%		**Volumized % of retail**	90%
Part Cost	$21.10		**Part Cost**	$10.00		**Part Cost**	$346.50
Overhead	8.5%		**Overhead**	8.5%		**Overhead**	8.5%
Component Cost	$22.89		**Component Cost**	$10.85		**Component Cost**	$375.95
Component 10: Purchased Ratchet Gear			**Component 11: Purchased Pawl**			**Component 12:Purchased Rack**	

Description	Metal Ratcheting Gear, 200mm OD, 20mm shaft diameter	**Description**	Pawl for 25 mm Wide Face Metal Ratcheting Gear	**Description**	Rack Track, 2m, Hardened Steel. CR30200
Vendor	McMaster-Carr	**Vendor**	McMaster-Carr	**Vendor**	Tuli
Retail Cost	$361.38	**Retail Cost**	$64.01	**Retail Cost**	$124.85
Units/yr.	3,923.00	**Units/yr.**	3,923.00	**Units/yr.**	3,923.00
Volumized % of retail	90%	**Volumized % of retail**	90%	**Volumized % of retail**	90%
Part Cost	$325.24	**Part Cost**	$57.61	**Part Cost**	$112.37
Overhead	8.5%	**Overhead**	8.5%	**Overhead**	8.5%
Component Cost	$352.89	**Component Cost**	$62.51	**Component Cost**	$121.92

Component 13: Purchased Pinion Gear		**Component 14: Purchased Pre-Filter**		**Component 15: Purchased Ball Valves**	
Description	SS Pinion Gear	**Description**	Large Particle Filter	**Description**	Ball Valves
Vendor	Grainger	**Vendor**	Amazon	**Vendor**	Assured Automation
Retail Cost	$246.40	**Retail Cost**	$81.24	**Retail Cost**	$568.00
Units/yr.	3,923.00	**Units/yr.**	3,923.00	**Units/yr.**	3,923.00
Volumized % of retail	90%	**Volumized % of retail**	90%	**Volumized % of retail**	90%
Part Cost	$221.76	**Part Cost**	$73.12	**Part Cost**	$511.20
Overhead	8.5%	**Overhead**	8.5%	**Overhead**	8.5%
Component Cost	$240.61	**Component Cost**	$79.33	**Component Cost**	$554.65

Table 2.4: Assembly Costs and Net Cost Calculation

Full Assembly		
Sub-Assembly 1: Piston	2	hrs
Sub-Assembly 2: Pilot-Operated Valve	0.5	hrs
Sub-Assembly 3: Membrane	2	hrs
Sub-Assembly 4: Ratchet/Rack&Pinion	2	hrs
Final Assembly:	2.5	hrs
Total Assy. Time	9	hrs
Labor Rate	60	$/hr
Labor Cost	540	
Overhead	35%	
Component Cost	729	

Misc. Data:	
Number of Assemblies:	3,923.00
Maintenance Hrs/Yr:	12.00
MARR (Minimum Attractive Rate of Return)	15%
Maintenance Cost ($/hr):	$ 60.00
Net Cost/Device:	$5,870.59
Net Capital Cost:	$25,109,509.77
Annual Maintenance Cost:	$ 2,824,560.00
US Inflation Rate	3.4%
Time to Deploy per device (hr):	0.5
Deployment Costs:	$117,690.00
Shipping:	$1,961,500.00

Table 2.5: Net Present Worth Analysis

Assume:	Useful Life of 5 Years		**Reference:**	US has $64 billion dollars of bottled water sales annually (2021)		
	Membrane Replacement every 2 years			Global Market $270 billion		
EOY	**Costs (A$)**	**Revenues (A$)**	**Net CF (A$)**	**Net CF (R$)**	**PW(A$)**	**PW(R$)**
0	$25,109,509.77	0	($25,109,509.77)	($25,109,509.77)	-$25,109,509.77	$ (25,109,509.77)
1	$ 2,824,560.00	$111,652,581.71	$108,828,021.71	$105,249,537.43	$94,633,062.35	$ 91,521,336.90
2	$ 3,837,502.65	$111,652,581.71	$107,815,079.06	$100,841,298.24	$81,523,689.27	$ 76,250,509.07
3	$ 2,824,560.00	$111,652,581.71	$108,828,021.71	$98,441,703.02	$71,556,190.82	$ 64,727,017.68
4	$ 3,837,502.65	$111,652,581.71	$107,815,079.06	$94,318,601.06	$61,643,621.38	$ 53,926,966.28
5	$ 2,824,560.00	$111,652,581.71	$108,828,021.71	$92,074,218.37	$54,106,760.54	$ 45,777,159.30
					Net Annual Cash Flow (A$)	**$111,652,581.71**
					Net PW (A$)	$338,353,814.58
					Net PW (R$)	$307,093,479.45

3 Technical Design

3.1 Evolution from Previous Competition

The previous years' designs contained or were heavily inspired by Batch Reverse Osmosis (BRO), an RO process where the brine is recirculated within the system, using pumps, which requires external energy.

This year's MECC team from Purdue also prioritized validating the PFRO process as part of its experimentation, on top of creating a novel WEC design for the MECC competition, while last year's team focused on creating a working pulley system to transfer power from the WEC to the BRO system. In light of the pressure requirements of PFRO, the team sourced components that were not only non-corrosive to seawater (such as buying the required fittings in stainless steel), but also resistant to fluctuations and highly pressurized water. Previous team's tested primarily with hydraulic oil and with regular, ideal wave profiles. This year, the team used saltwater and an irregular wave profile to evaluate the system's performance. Moreover, last year's team used a motor to validate their experiments and hypotheses. The current team integrated a 3-phase AC motor with a positive displacement pump to control the flow within the system.

The main advancement is the upgrade from the BRO to the PFRO process, whose main advantages in the design include purely-mechanical and not including electrical components such as solar panels.

3.2 Proposed Design and Objective

Mentioned before, the proposed solution is a ***Wave-Powered Pulse Flow Reverse Osmosis Desalination System***. Utilizing the rising and falling energy of ocean waves, it causes a buoy to rise and fall. A wave energy converter then uses that energy to actuate a piston back and forth, pressurizing seawater. Pressurized seawater then enters a reverse osmosis membrane, converting seawater into clean, drinkable water utilizing the novel desalination technique of pulse flow reverse osmosis (PFRO). The design will be a purely mechanical design, meaning that the system will be able to desalinate water without any electrical components. This greatly reduces maintenance requirements as well as increases robustness and simplicity.

The system consists of 3 main components: the buoy, the wave energy converter, and the pulse reverse osmosis system. To begin with the buoy, a polyethylene shell is used to house all the components. The buoy is then anchored to the seafloor. As the waves rise and fall, the buoy will rise and fall alongside it, shown by Figure 3.1.

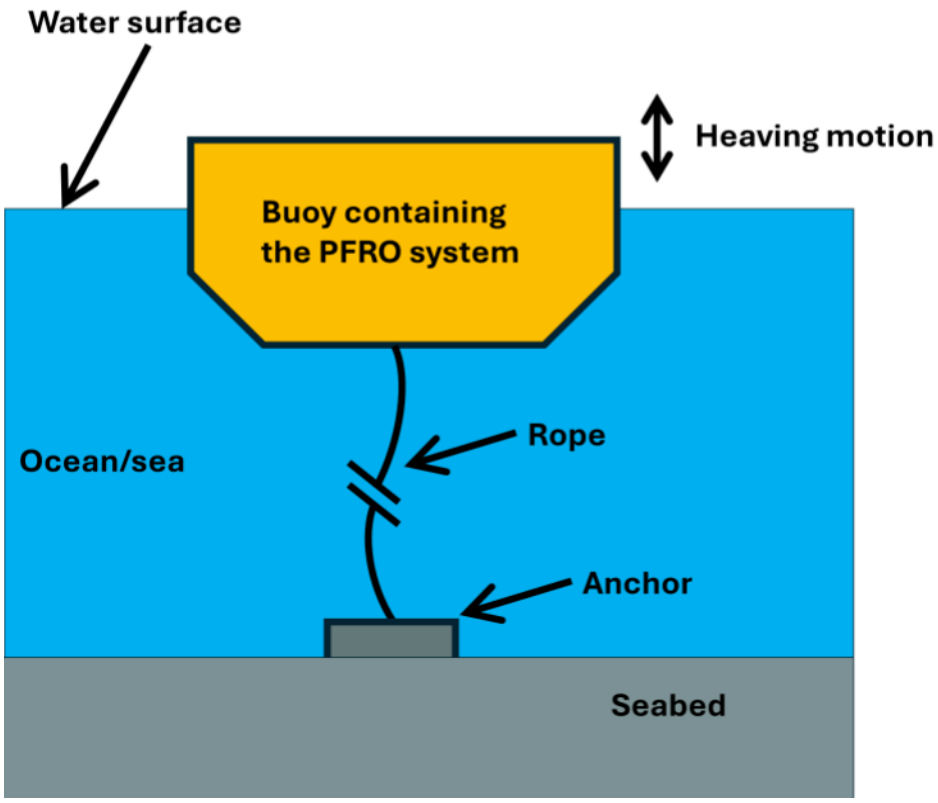

Figure 3.1: External Buoy Diagram

Within the buoy, it houses both the wave energy converter (WEC) as well as the PFRO system. Beginning with the WEC, Figure 3.2 depicts how the system is able to harness ocean wave movement into water.

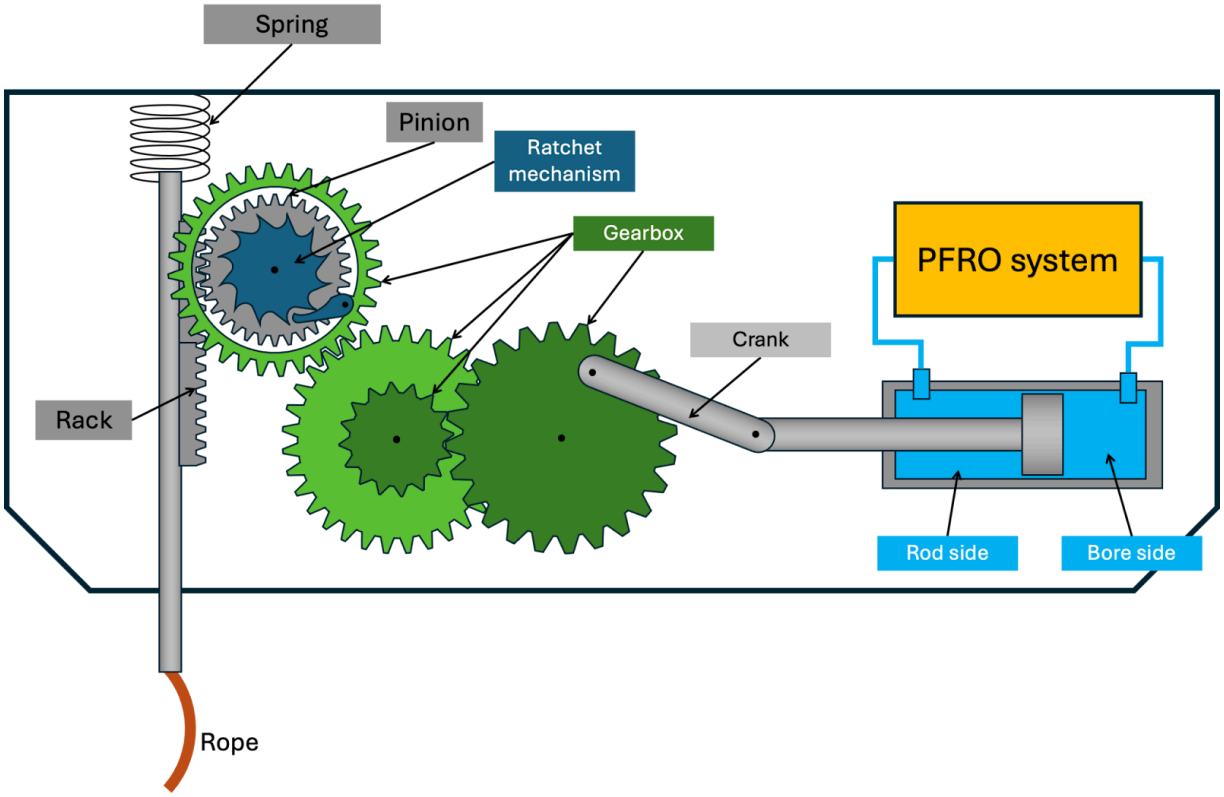

Figure 3.2: Wave Energy Converter Diagram

Starting at the left, a rack can be seen connected to a spring and a rope. A pinion is meshed with the rack and constrained to the buoy. As the buoy rises, the rope gradually straightens until it becomes fully taut. As a result, the rack will stay at a constant height while the pinion rises, causing the pinion to rotate counterclockwise. As the buoy falls, the rack and pinion system does the opposite. The spring that was once extended will pull the rack upwards while the pinion lowers, causing the pinion to rotate clockwise. Through the rack and pinion mechanism, the linear motion of the rising and falling of waves is able to be converted into the counterclockwise and clockwise motion of the pinion, respectively.

From there, a ratchet is connected to the pinon and a pawl is connected to an outer gear. As the pinion rotates counterclockwise, the pawl will catch the teeth of the ratchet, causing the outer gear to spin counterclockwise. However, as the pinion rotates clockwise, the pawl will not catch, allowing for the pinion to free spin and the outer gear remains stationary. The ratchet mechanism is able to limit the system to only spin in one direction: counterclockwise.

Next, the outer gear is connected to a gearbox, establishing gear reduction. This greatly reduces the revolutions per minute (RPM) while increasing the torque output - preventing rapid oscillations in piston movement and ensuring that the system only completes full cycles. Finally, the last gear connected to a crank and piston, converting the rotational motion of the gear into a

linear, back and forth motion of the piston. As the piston moves back and forth, seawater in both chambers of the piston (rod and bore side) becomes pressurized and enters the PFRO system.

In summary, the objective of the design is to utilize a wave energy converter that is able to harness the energy of rising and falling ocean waves into pressuring seawater in a piston, which will flow into the PFRO system.

3.3 Pulse Flow Reverse Osmosis Background

Before getting into the PFRO system, it is first essential to understand pulse flow reverse osmosis conceptually. Pulse flow reverse osmosis is broken down into two major phases: a permeate phase and flushing phase. During the permeate phase (Figure 3.3), pressurized seawater enters the reverse osmosis (RO) membrane while the brine output is completely blocked. As a result, all the seawater entering the RO membrane gets filtered to clean drinking water (permeate), meaning a 100% recovery ratio is achieved. However, as more and more seawater gets filtered by the RO membrane, the brine buildup within the membrane becomes increasingly salty, reaching supersaturation. At this point, the system switches to the flushing phase. During the flushing phase (Figure 3.4), pressurized seawater continues to enter the RO membrane except now the brine output is open. This enables the supersaturated brine to flush out of the system and be replaced by new seawater. Because the brine port is completely open, no permeate is produced, meaning a 0% recovery ratio is achieved. The PFRO cycle then repeats, toggling between the permeate and flushing phases.

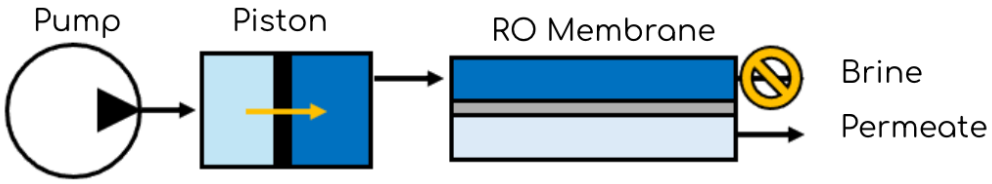

Figure 3.3: Permeate Phase of Pulse Flow Reverse Osmosis

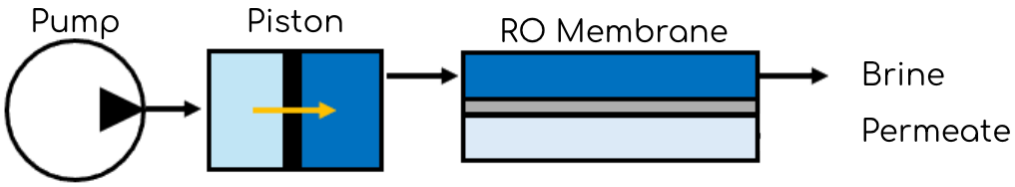

Figure 3.4: Flushing Phase of Pulse Flow Reverse Osmosis

A major benefit of a PFRO cycle is a more power efficient desalination process compared to conventional continuous reverse osmosis. Unlike continuous reverse osmosis which uses a constant maximum pressure, PFRO varies its pressure input based on salinity. Therefore, by constantly adjusting pressure inputs in response to increasing salinity levels, PFRO optimizes energy consumption during the desalination process, allowing the system to operate efficiently

without constantly exerting maximum pressure, unlike conventional continuous reverse osmosis. Another benefit of PFRO is the lower risk of biofouling. Biofouling is the slow accumulation of organic matter from the seawater in the membrane that operates to decrease the membrane's efficiency. In continuous reverse osmosis, the pressure and salinity conditions within the RO membrane are fairly constant, allowing for bacteria and algae to grow. However, with PFRO, the rapid fluctuations of the pressure and salinity with each cycle make it significantly harder for these microorganisms to produce. This reduces biofouling and extends the RO membrane's lifespan significantly. A membrane in a PFRO system could last four years, whereas a membrane in a continuous system often lasts less than half that time. Another major benefit of PFRO is its simplicity and robustness. Unlike other systems, such as batch reverse osmosis which rely on an additional circulation pump, PFRO simply closes and opens the brine output. Given that the device will be subjected to all the variable forces of the ocean, it is critical for the system to be robust enough to withstand these conditions while also requiring minimal maintenance. Lastly, the largest reason why PFRO decided is because of its wave energy conversion compatibility. Given that the PFRO system can be powered by a pressurized piston, it can be perfectly combined with the WEC described above (Figure 3.2) since their output involves piston actuating back and forth and their input requires only wave energy.

3.4 Pulse Flow Reverse Osmosis System Design

Figure 3.5 illustrates the final PFRO system, showcasing the system's fully passive and mechanically driven operation. The check valves below only allow flow to go one direction (circle side) and prevent from. The flow line symbolizes the water flow in the system. The pilot line is a controller line that controls a system given a certain pressure output. In this scenario, the pilot line is connected to the pilot operated (PO) check valve. Normally, if the pilot port does not detect any pressure, the PO check valve will remain closed. However, if the pilot port detects pressure, the PO check valve will open.

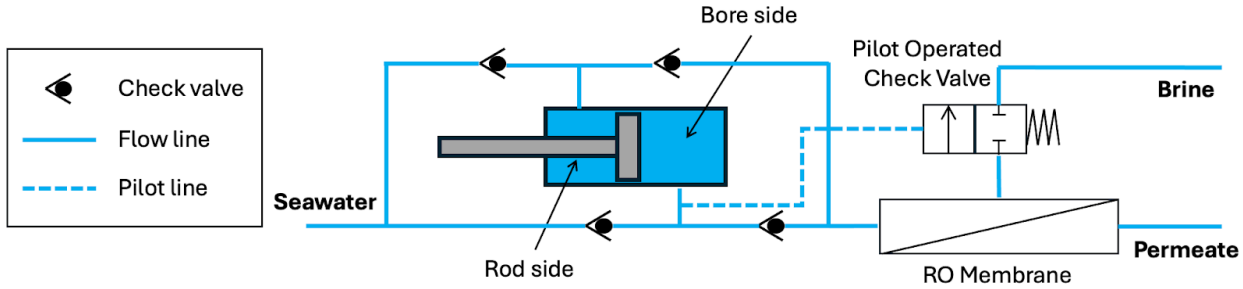

Figure 3.5: PFRO System

During the permeate phase (Figure 3.6), the piston is extending, pressurizing the rod side chamber. Through a series of check valves, inlet seawater would flow into the low-pressure bore side of the cylinder and feed seawater would flow into the membrane. Examining the pilot-operated check valve (PO valve), the valve will only allow flow through if the pilot line

reads a high pressure. Because the pilot line is connected to the low-pressure bore side, the PO valve will not open, blocking the brine output of the membrane. Because the brine output is blocked, it allows for pressure to build up inside the membrane as the piston continues to extend, producing fresh water level rises, ultimately producing pure water at an efficient rate.

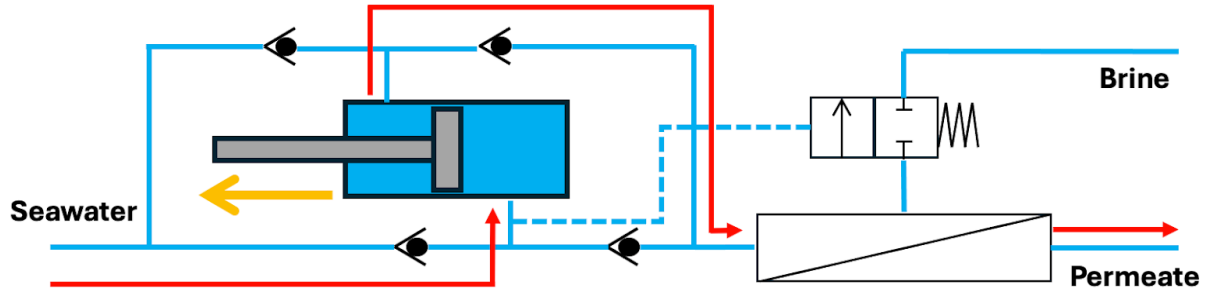

Figure 3.6: PFRO System in Permeate Phase

During the flushing phase (Figure 3.7), the piston is compressing, pressurizing the bore side chamber. Through a series of check valves, inlet seawater would flow into the low-pressure rod side of the cylinder and feed seawater would flow into the membrane. However, in this case, because the bore side of the chamber is pressurized, the PO valve will read a high pressure, opening the brine output and allowing the supersaturated brine to flush. As a result, the previously stored brine inside the membrane is released, outputting high-pressure brine.

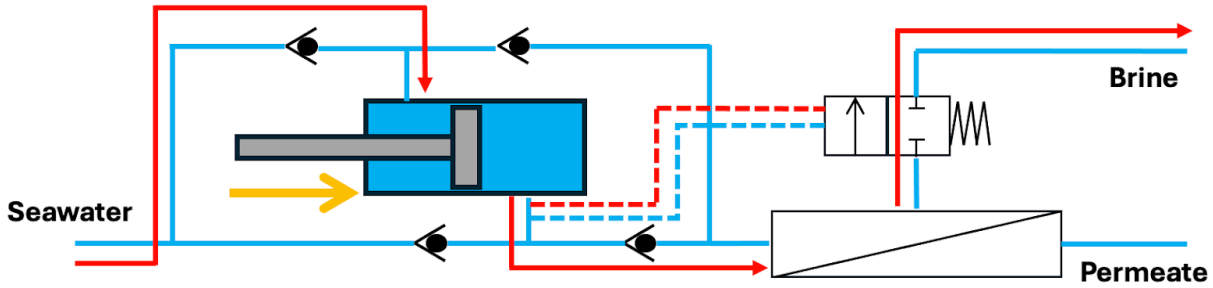

Figure 3.7: PFRO System in Flushing Phase

3.5 Performance Analysis

Numerous forms of analysis were conducted to understand the scope of the project, and to ground the design of the PFRO product in relevant data. The first data that was obtained was buoy data from San Juan, Puerto Rico, to understand the average wave characteristics in the area. After analyzing the trends of the significant wave height and the periods of the waves from data from National Data Buoy Center (US Department of Commerce), leading to a significant wave height of 2 meters and wave period of 8 seconds.

For the WEC sub-system, the Purdue MECC team considered the passive mechanical system best in power transmission from the waves to the PFRO system, as power conversion between mechanical to electrical to mechanical would result in significant power losses and inefficiencies. Adhering to the passive system would also mean that there would be a lower reliance on other power generation means, such as solar panels, hence reducing the maintenance requirement when the PFRO system is successfully deployed.

This would be similar to the technology implemented by Oneka Technologies, that also does not use any electricity in their products, but transfers the energy from their WEC system to a continuous RO system. Less energy and power would be required in the PFRO system implementation, as the water does not need to be pressurized to a constant pressure and can slowly be ramped up, based on the movement of the waves and the force transferred through the WEC system.

3.5.1 Power Analysis

A power analysis is conducted to determine the energy required to desalinate water. As the system is purely mechanical, there will be no losses converting from electrical to mechanical and vice versa. However, due to the nature of the ratchet mechanism, the system will only run when the wave is rising. Assuming the average amplitude of the rising and falling of the waves are the same, a 50% power efficiency is determined as only half of the energy from the waves (rising) is utilized. Furthermore, loss of efficiency due to friction in the piston and pipes can also be determined.

Exploring the power efficiency per amount of water produced, Equation 1 is utilized.

$$\text{Equation 1: Power} = P * Q$$

Here, P stands for pressure and Q stands for flow rate. Calculating conservatively, it is first assumed that 70 bar is required to desalinate seawater. Next, given the system requirements that it will ideally produce 1 L/min, the final power output is calculated to be 116.67 W to produce 1 L/min. In terms of energy, using Equation 2, it is determined that 7000 J is required to produce 1 L of fresh water.

$$\text{Equation 2: Energy} = \text{Power} * t$$

3.5.2 Crank Arm Mechanical Loading Analysis

Next, the team explored the piston driving mechanism; the crank arm assembly. Initially, the aim was to purchase a commercially available assembly, however the unique stroke length and high torque requirements made this unfeasible. Thus, the team began design on a custom crank arm system divided into two key components: the driver arm and the connecting arm.

First, the shaft length design constraints were determined. In order to prevent piston damage from over extension, it was decided that the overall extended length of the crank arm system should not exceed 75% of the stroke length. With this and the learnings from the prototyping phase, the driving arm length, r, was determined to be 4.04”, and the connecting arm was chosen to be 1.5r, which is henceforth referred to as l - 6.07”. Two connecting arms will be used to “sandwich” the piston arm. This will prevent torsion along the shaft. Both parts are pictured in Figure 3.8 and 3.9.

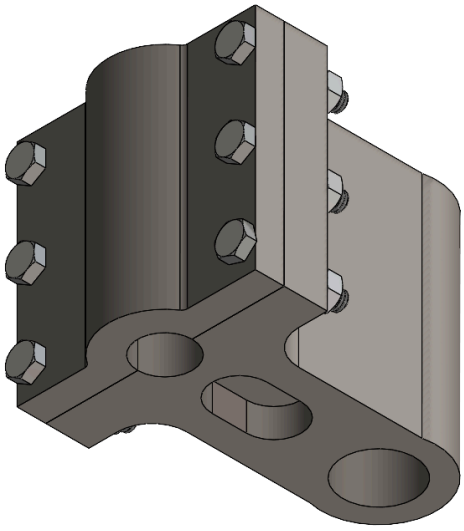

Figure 3.8: Driver Arm CAD

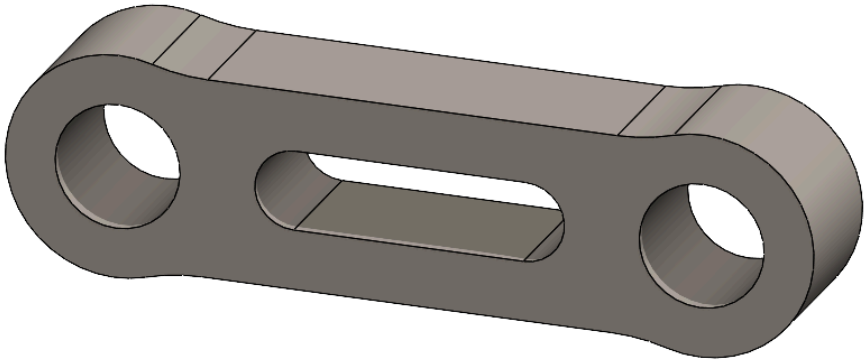

Figure 3.9: Connecting Arm Subsystem CAD

With these values determined, the maximum torque the system would need to supply was characterized using the maximum possible pressure of the system - 69 bar - and by extension the maximum force. To calculate the maximum force the system experiences, the team used the

calculations seen below. The system was designed to support this maximum torque value - 3,800 N-m - without failure. The intention is that the system never sees this maximum torque value, but the parts be engineered to sustain it in case of overpressurization. Both manufactured parts have factors of safety (FS) above 2.0. Finite element analysis (Figure 3.12-3.17) was used to confirm these design features.

Maximum Force and Torque Calculations

Known:

Piston Area, Rodside: $A_{Rod} = 0.0044\ m^2$

Maximum Piston Pressure: $P_{max} = 69\ bar = 69 * 10^5\ Pa$

Driver Arm Length: $r = 0.1028\ m$

Connecting Arm Length: $l = 0.1542\ m$

Sketch:

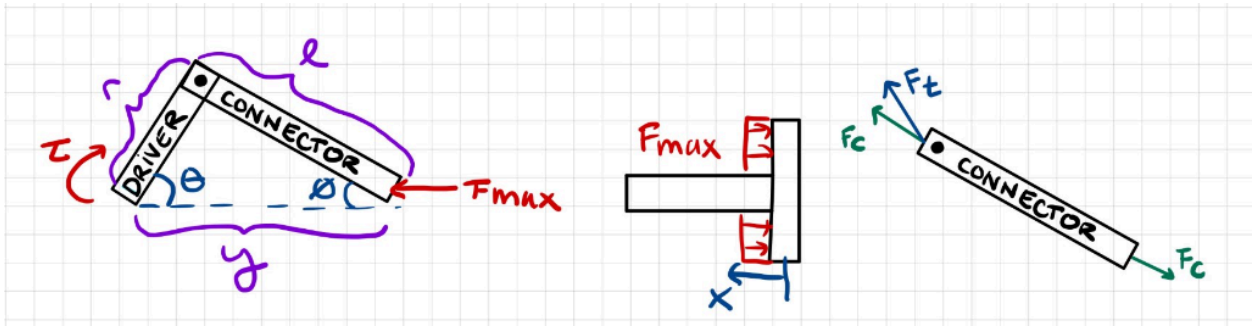

Figure 3.10: Sketch for Crank Arm Calculations

Assume:

- The reaction force needed to pressurize the piston is constant
- Transient state (Θ, ϕ vary with time)
- Force due to torque (Ft) is not perfectly perpendicular to the connector arm

Using geometry and trig identities (forming 2 right triangles with the crank arm):

$$\text{Equation 3: } F_c = \frac{F_{max}}{cos\phi}$$

$$\text{Equation 4: } F_t = F_c sin(\phi + \theta)$$

$$\text{Equation 5: } \tau = F_t * r = \frac{r * F_{Max}}{cos\phi} sin(\phi + \theta)$$

$$\text{Equation 6: } \frac{sin(\phi+\theta)}{cos\phi} = sin\theta + cos\theta tan\phi$$

$$\text{Equation 7: } sin\phi = \frac{r}{l} sin\theta$$

Equation 8: $tan\phi = \frac{sin\phi}{\sqrt{1-sin^2\phi}} = \frac{\frac{r}{l}sin\theta}{\sqrt{1-(\frac{r}{l}sin\theta)^2}}$

$$\Rightarrow \tau = r * F_{max}(sin\theta + cos\theta \frac{\frac{r}{l}sin\theta}{\sqrt{1-(\frac{r}{l}sin\theta)^2}})$$

$$F_{max} = A_{rodside} * P_{max} = 30,271\ N$$

The expression for torque was then graphed across $\theta = [0, \pi]$, using MATLAB, which corresponds to 1 phase of the piston cycle. At approximately $\theta = 65°$, the maximum torque occurs: $\tau \approx 3800\ N - m$.

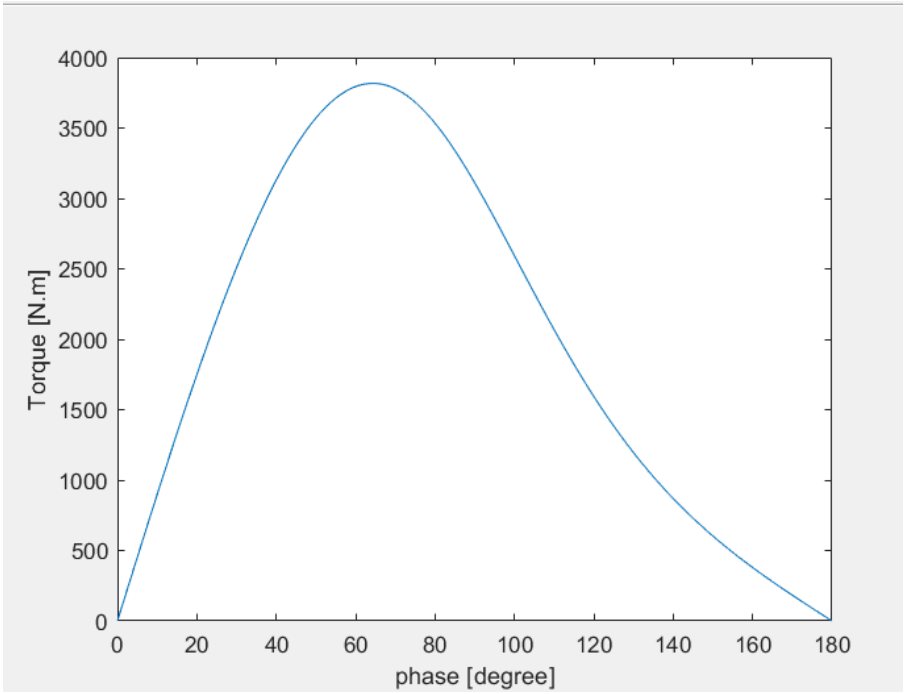

Figure 3.11: Crank Arm Torque vs. Phase in Degrees

This value will be used to ensure the crank-arm parts are designed with an adequate factor of safety.

3.5.3 Crank Arm FEA Analysis

Connecting Arm

Assume: 1045 Carbon Steel, Static torque, Equally distributed load ($\tau = 0.5 * \tau_{max}$), Did not consider fastener effects

Boundary Conditions:

1. Left (x = 1”) : $\tau = 1900\,N - m$
2. Right (x = 6”): Fixed End

Results:

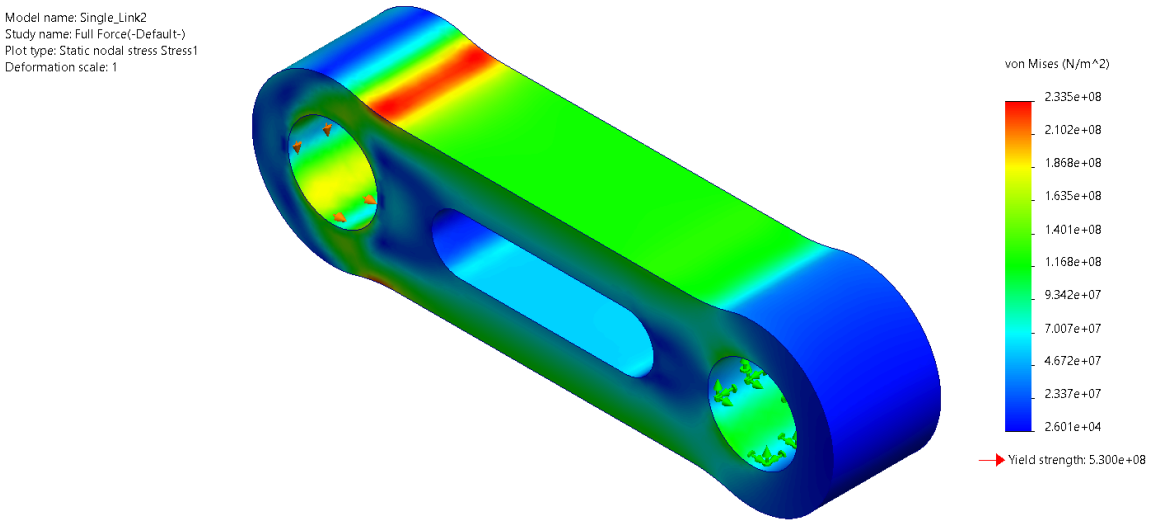

Figure 3.12: Von Mises Stress Contour - Connecting Arm

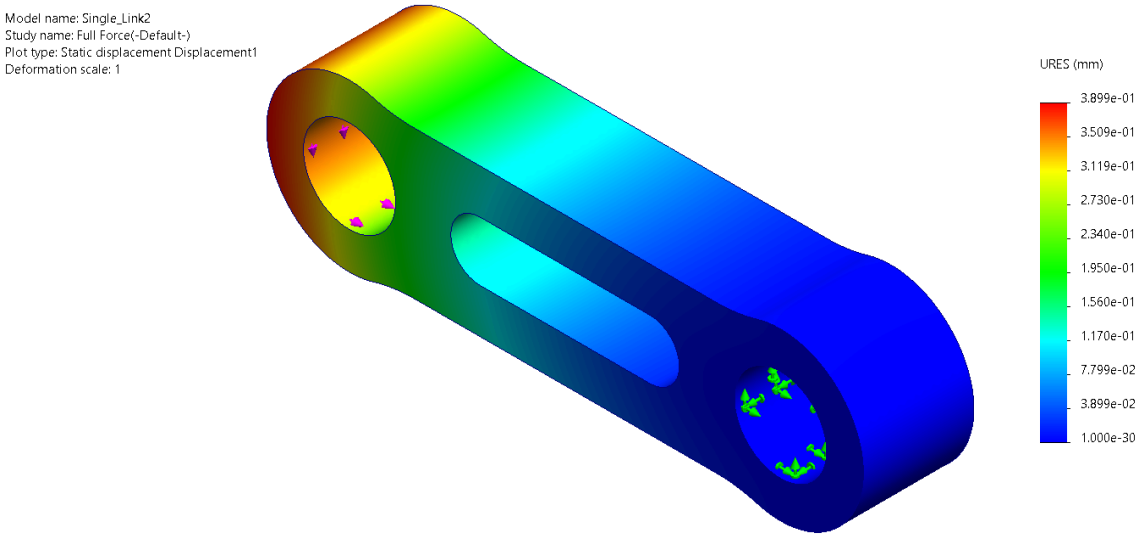

Figure 3.13: Displacement Contour - Connecting Arm

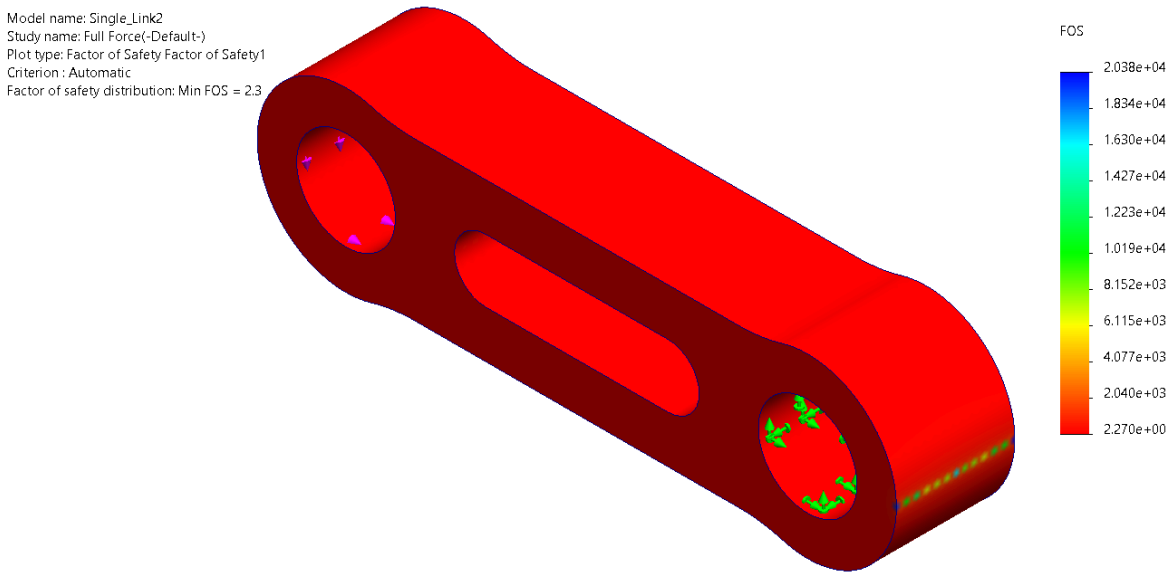

Figure 3.14: Factor of Safety Contour - Connecting Arm

Discussion:

The current design has a minimum FS of 2.3, meaning it can safely support double the maximum load before yielding. The displacement is small and the team has identified locations of maximum stress: the filets close the ends. Thus, the part is safe for the team's applications, but should be observed carefully for signs of stress at these key locations.

Driver Arm

Assume: 1045 Carbon Steel, Static torque, Full load ($\tau = \tau_{max}$), Did not consider fastener effects

Boundary Conditions:

1. Left (x = 1") : $\tau = 3800\ N - m$
2. Right (x = 4"): Fixed End

Results:

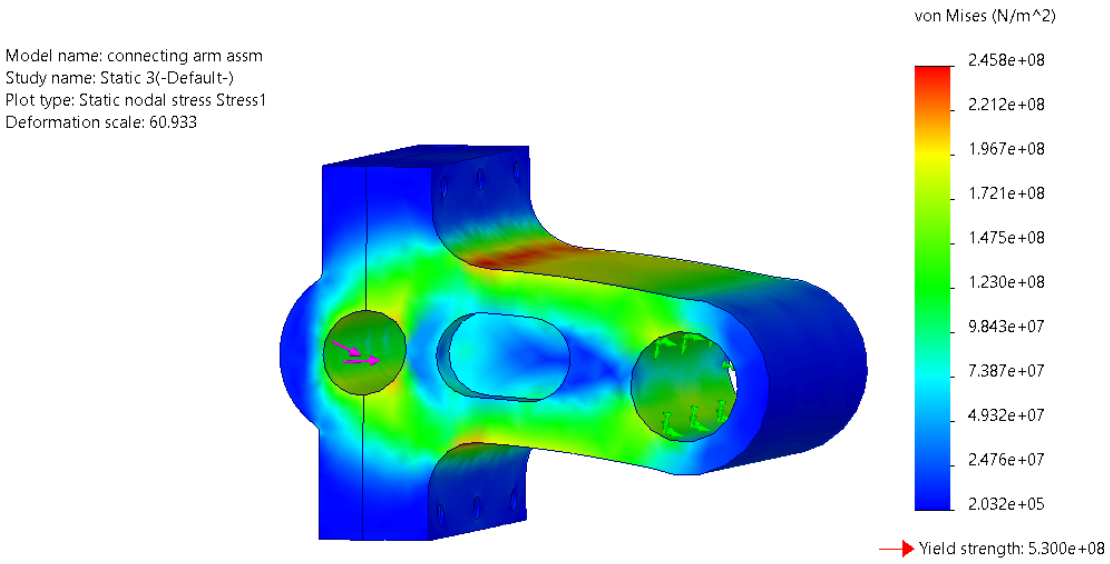

Figure 3.15: Von Mises Stress Contour - Driver Arm

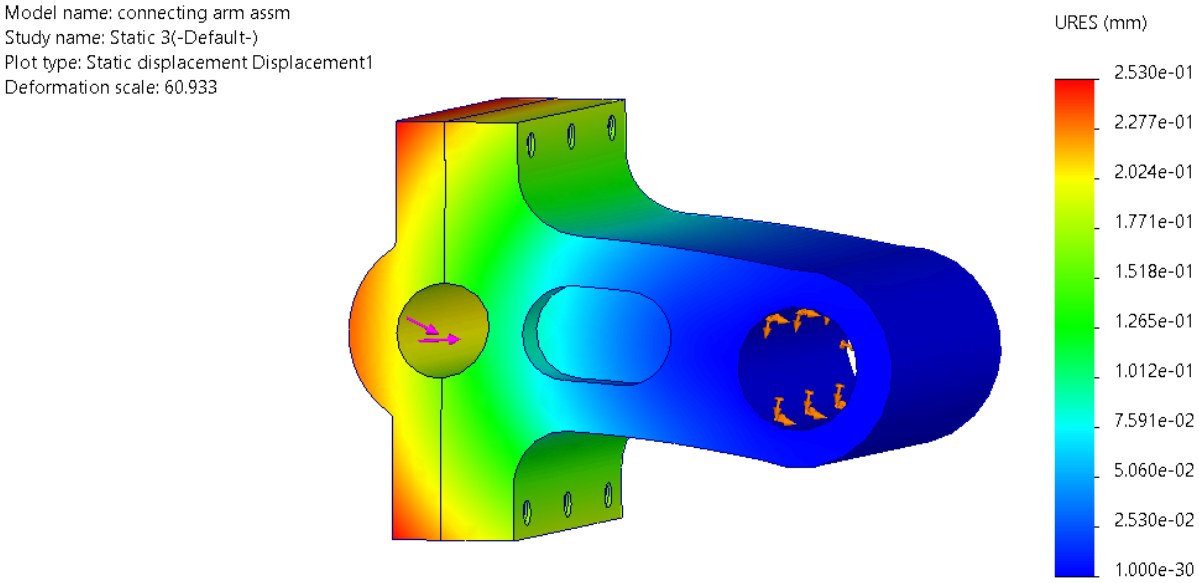

Figure 3.16: Displacement Contour - Driver Arm

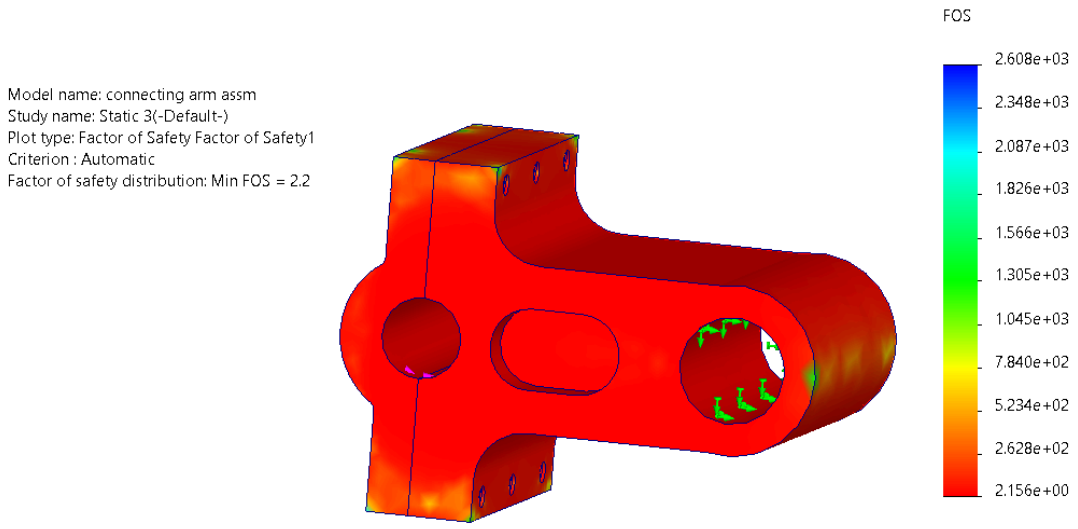

Figure 3.17: Factor of Safety Contour - Driver Arm

To connect and support the assembly, a myriad of purchased parts are used. These include needle-roller bearings, a sleeve bearing, clevis pins, hex bolts, nuts, a threaded rod end to connect to the piston shaft, and an aluminum bushing to maintain lateral movement. All of these parts have been evaluated for the FS under maximum load using the manufacturer's published statistics. A complete table of these values is represented in Table I1. The current design has a minimum FS of 2.2, meaning it can safely support double the maximum load before yielding.

Table 3.1: Factors of Safety for Parts in Crank Arm Assembly

Part	**Factor of Safety**	**Material**
Driving Arm	2.2	1045 Carbon Steel
Connecting Arm	2.3	1045 Carbon Steel
Bolts	13	18-8 Stainless Steel
Needle-Roller Bearings	1.3	Steel
Sleeve Bearings	1.8	932 Bronze
9" Pin	5.3	1045 Carbon Steel
4.7" Pin	5.3	1045 Carbon Steel

Given all these analyses, the full assembly is shown in Figure 3.18.

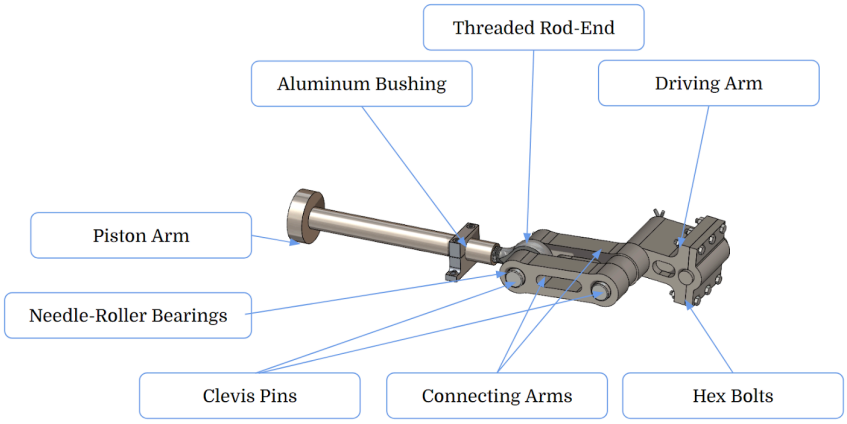

Figure 3.18: Crank arm CAD assembly

3.5.4 Buoy Mechanical Loading Analysis

Next, regarding the buoy, WEC-Sim was used to analyze the forces acting on the body of the buoy, by running simulations of the buoy in water. WEC-Sim has the following prerequisite files to run the simulation:

- Geometry of the object (.stl, ASCII format)
- Hydrodynamics and hydrostatics coefficients (.h5 format)
- Wave Input Data (.mat format)
- Constraints of the body involved modeled through Simulink (.slx format)

Given the constraints posed by the final RO design, a buoy was designed on SolidWorks as a shell frustum of a cone, with the major radius being 6ft and the minor radius being 3ft, with a height of 3ft. The buoy's material was set as high-density polyethylene (HDPE) due to its strength and low density, and the wall thickness was set to ⅜ inches.

Static buoyancy analysis was done to determine the immersed depth of the buoy, by equating the dimensions of the frustum to the height, and equating the mass of the buoy and an estimated mass of the RO system to the mass of the displaced volume. This resulted in a water depth of 0.1451m (roughly 0.5ft).

```
%constants
rho_metric = 1025; %kg/m3
buoy_mass_kg = 72.7; %kg
RO_mass_kg = 50;     %kg
r_feet = 1.5;        %ft
theta = asind(1.5/2.5); %degrees
h_feet = 0:0.001:2;
g  = 9.81; %metric

%equations that define relations in the frustum base of buoy
R_feet = h_feet.*tand(theta) + r_feet;
Volume_ft3 = (pi .* h_feet ./ 3) .* (R_feet.^2 + R_feet.*r_feet + r_feet^2);

Volume_req_m3 = (buoy_mass_kg + RO_mass_kg) / rho_metric;
Volume_req_ft3 = Volume_req_m3 * 35.3147;

%Determining the height and major radius of the frustum immersed in the
%water based on buoyancy
[Volume_val index] = min(abs(Volume_req_ft3 - Volume_ft3));
R_val_feet = R_feet(index);
h_val_feet = h_feet(index);
R_val_m = R_val_feet / 3.281
h_val_m = h_val_feet / 3.281
```

```
R_val_m =

    0.5660


h_val_m =

    0.1451
```

Figure 3.19: MATLAB Code to Determine Immersed Buoy Length

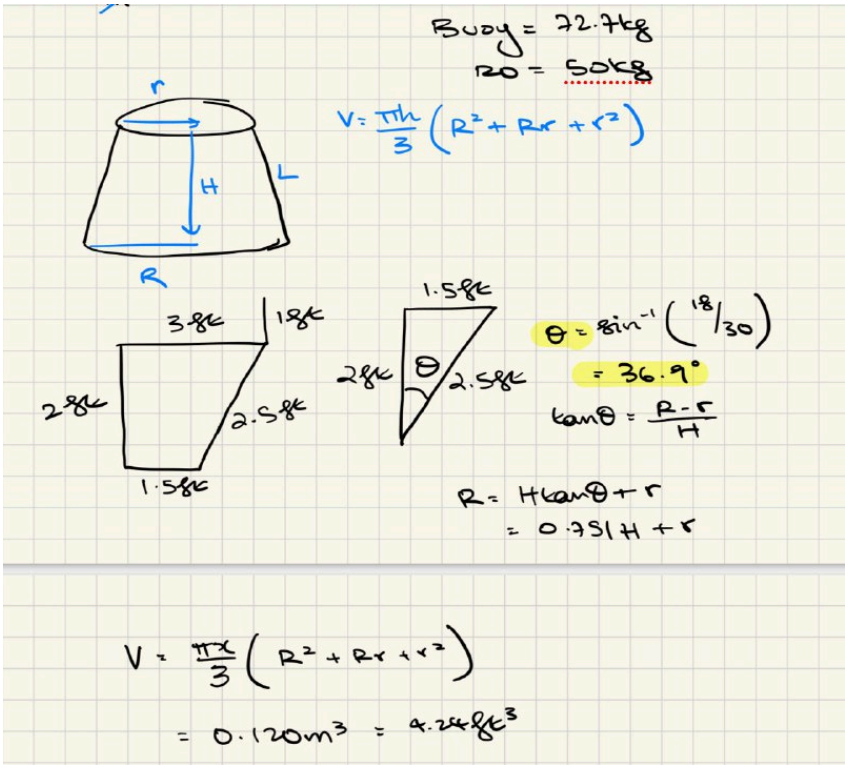

Figure 3.20: Handwritten Derivations of MATLAB Equations

- $V = \frac{\pi h}{3}(R^2 + Rr + r^2)$
- $R = Htan\theta + r$

An average wave period of 8 seconds and a significant wave height of 2 meters were used to find the relevant coefficients. There are several established boundary element methods (BEM) and programs to obtain the required hydrodynamic data, such as NEMOH, Capytaine, WAMIT, and Aqwa that WEC-Sim recognizes. A challenge encountered was the lack of approachable documentation for this process.

Another program, called BEMRosetta, was used to import the buoy mesh and output it as a .dat file, which is recognized by the BEM programs. It was also used to adjust the water line and extract the submerged part of the buoy (which will be referred to as the hull). NEMOH was then used to extract the relevant hydrodynamic and hydrostatic coefficients with 6 degrees of freedom for translational and rotational movements in the three axes. This data was converted to a .h5 file format.

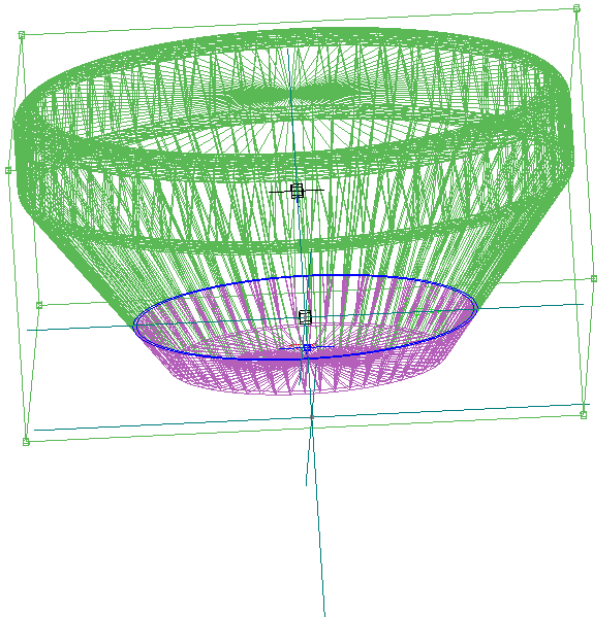

Figure 3.21: BEMRosetta View of Buoy Mesh (green) and Hull (purple)

The WEC-Sim input file was then adjusted to output an irregular wave with the wave parameters mentioned earlier, using an in-built algorithm that uses the Pierson-Moskowitz (PM) wave spectrum. The PM wave spectrum was used in place of the JONSWAP spectrum as the team maintained an assumption of the sea being fully developed in the waters near San Juan. The irregular wave class was used to make the simulation as realistic as possible, since waves are

generally irregular. More modifications of parameters were done, such as the mass of the displaced fluid, the moments of inertia of the buoy, as well as the type of constraint experienced.

```
--- Environment
------------------------------------------------------------------------------------------------------------
1025.0              ! RHO             ! KG/M**3   ! Fluid specific volume
9.81                ! G           ! M/S**2    ! Gravity
0.                ! DEPTH         ! M     ! Water depth
0.  0.            ! XEFF YEFF     ! M     ! Wave measurement point
--- Description of floating bodies
------------------------------------------------------------------------------------------------------------
1                 ! Number of bodies
--- Body 1
------------------------------------------------------------------------------------------------------------
buoy6\mesh\buoy6.dat            ! Name of mesh file
256 250           ! Number of points and number of panels
6                 ! Number of degrees of freedom
1 1. 0. 0. 0. 0. 0.     ! Surge
1 0. 1. 0. 0. 0. 0.     ! Sway
1 0. 0. 1. 0. 0. 0.     ! Heave
2 1. 0. 0. 0. 0. -7.5       ! Roll about CdG
2 0. 1. 0. 0. 0. -7.5       ! Pitch about CdG
2 0. 0. 1. 0. 0. -7.5       ! Yaw about CdG
6                 ! Number of resulting generalised forces
1 1. 0. 0. 0. 0. 0.     ! Force in x direction
1 0. 1. 0. 0. 0. 0.     ! Force in y direction
1 0. 0. 1. 0. 0. 0.     ! Force in z direction
2 1. 0. 0. 0. 0. -7.5       ! Moment force in x direction about CdG
2 0. 1. 0. 0. 0. -7.5       ! Moment force in y direction about CdG
2 0. 0. 1. 0. 0. -7.5       ! Moment force in z direction about CdG
0               ! Number of lines of additional information
--- Load cases to be solved
------------------------------------------------------------------------------------------------------------
10  0.1 1.0     ! Number of wave frequencies, Min, and Max (rad/s)
1   0.  0.      ! Number of wave directions, Min and Max (degrees)
--- Post processing
------------------------------------------------------------------------------------------------------------
1   0.1 10.     ! IRF               ! IRF calculation (0 for no calculation), time step
and duration
1                 ! Show pressure
0.  0.  180.        ! Kochin function       ! Number of directions of calculation (0 fo
no calculations), Min and Max (degrees)
10  10  100.    100.    ! Free surface elevation    ! Number of points in x direction (
for no calcutions) and y direction and dimensions of domain in x and y direction


```

Figure 3.22: Nemoh.cal file To Run NEMOH

The simulation was then conducted with 3 degrees of freedom, resulting in irregular wave amplitudes and force readings fluctuating between +/- 140N acting on the buoy. An assumption was made that all the force experienced by the body would get transferred to the piston assembly. Further assumptions and considerations were made, such as the buoy floating in the water without any mooring mechanisms. For further study, MoorDyn would be implemented with the WEC-Sim simulations to obtain better force analyses.

Simulation Data

```
simu = simulationClass();              % Initialize Simulation Class
simu.simMechanicsFile = 'MECC_Buoy.slx';      % Specify Simulink Model File
simu.mode = 'normal';                  % Specify Simulation Mode ('normal','accelerator','rapid-accelerator')
simu.explorer = 'on';                  % Turn SimMechanics Explorer (on/off)
simu.startTime = 0;                    % Simulation Start Time [s]
simu.rampTime = 10;                   % Wave Ramp Time [s]
simu.endTime = 100;                  % Simulation End Time [s]
simu.solver = 'ode4';                  % simu.solver = 'ode4' for fixed step & simu.solver = 'ode45' for variable step
simu.dt = 0.01;                                              % Simulation time-step [s]
simu.cicEndTime = 1;
simu.rho = 1025;
```

```
WEC-Sim: An open-source code for simulating wave energy converters
Version: 6.0

Initializing the Simulation Class...
```

Figure 3.23: Simulation Data Parameters in WEC-Sim

Wave Information

% noWaveCIC, no waves with radiation CIC waves = waveClass('noWaveCIC'); % Initialize Wave Class and Specify Type

```
% % Regular Waves
%waves = waveClass('regular');           % Initialize Wave Class and Specify Type
%waves.height = 2;                      % Wave Height [m]
%waves.period = 8;                        % Wave Period [s]

% % Regular Waves with CIC
% waves = waveClass('regularCIC');          % Initialize Wave Class and Specify Type
% waves.height = 2.5;                       % Wave Height [m]
% waves.period = 8;                         % Wave Period [s]

% % Irregular Waves using PM Spectrum
  waves = waveClass('irregular');           % Initialize Wave Class and Specify Type
  waves.height = 2.5;                       % Significant Wave Height [m]
  waves.period = 8;                         % Peak Period [s]
  waves.spectrumType = 'PM';                % Specify Wave Spectrum Type
  waves.direction=[0];
```

Figure 3.24: Wave Information Parameters in WEC-Sim

Body Data

Float

```
body(1) = bodyClass('hydroData/buoyhull.h5');
    % Create the body(1) Variable, Set Location of Hydrodynamic Data File
    % and Body Number Within this File.
body(1).geometryFile = 'geometry/buoy.stl';    % Location of Geomtry File
body(1).mass = 122.7;
    % Body Mass. The 'equilibrium' Option Sets it to the Displaced Water
    % Weight.
body(1).inertia = [25.96 25.96 36.96];  % Moment of Inertia [kg*m^2]
```

Figure 3.25: Body Data of Buoy in WEC-Sim

PTO and Constraint Parameters

Floating (3DOF) Joint

```
constraint(1) = constraintClass('Constraint1'); % Initialize Constraint Class for Constraint1
constraint(1).location = [0 0 0]; % Constraint Location [m]

% Translational PTO
%pto(1) = ptoClass('PTO1');                    % Initialize PTO Class for PTO1
%pto(1).stiffness = 0;                         % PTO Stiffness [N/m]
%pto(1).damping = 1200000;                     % PTO Damping [N/(m/s)]
%pto(1).location = [0 0 0];                    % PTO Location [m]
```

Figure 3.26: 3 DOF Constraint data in WEC-Sim

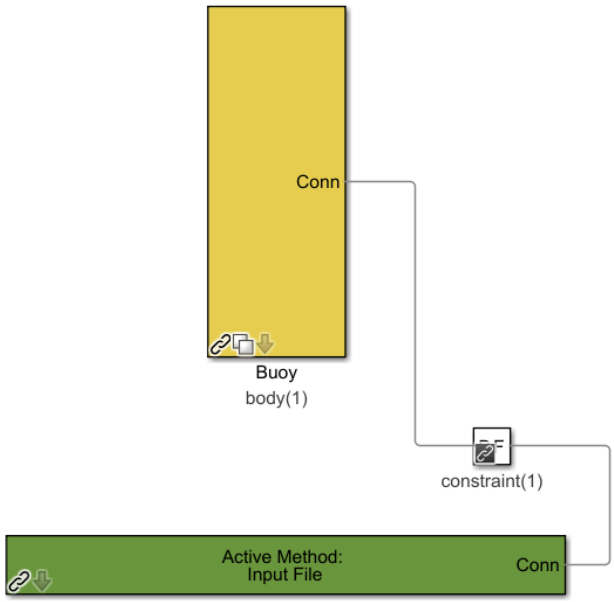

Figure 3.27: Simulink diagram for WEC-Sim

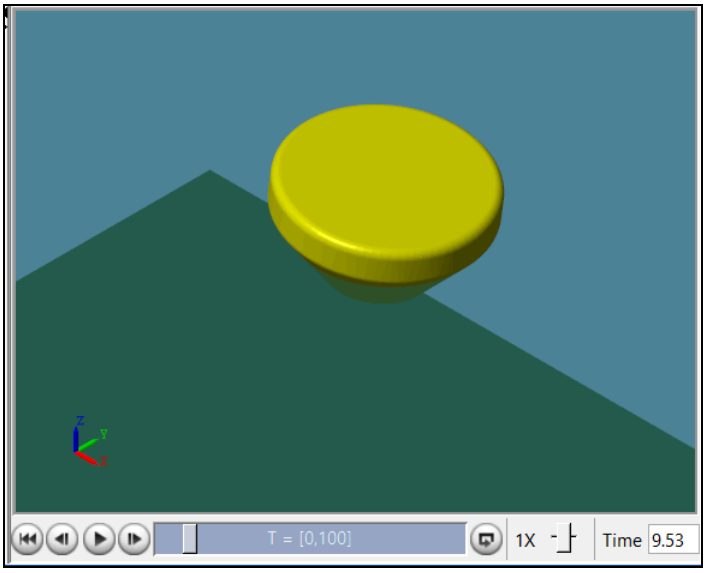

Figure 3.28: Buoy modeled on WEC-Sim, visualized through MATLAB Simscape Multi-Body

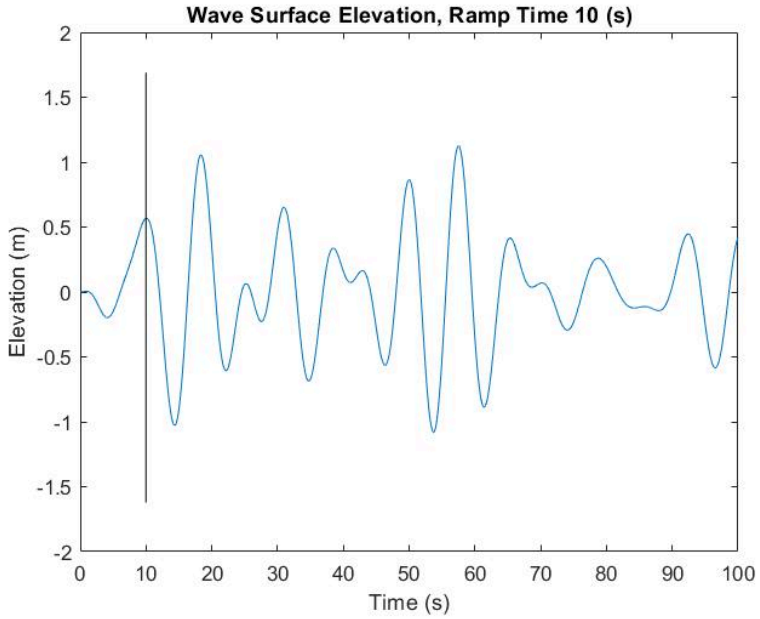

Figure 3.29: Irregular wave elevation data from WEC-Sim

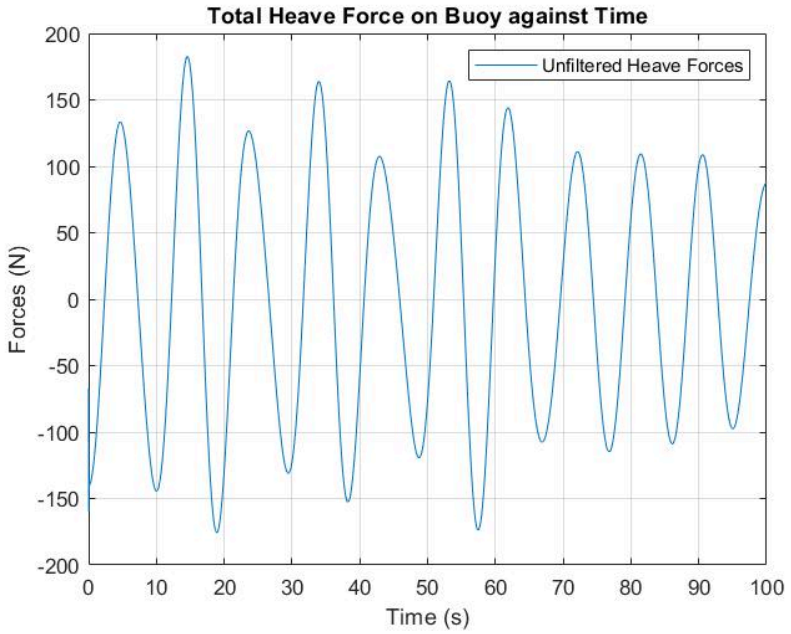

Figure 3.30: Heave Forces on Buoy from WEC-Sim

From the WEC-Sim simulations, the team was able to obtain the irregular wave surface elevation as well as the heave forces acting on the buoy. This served as a baseline to understand the forces and the displacement experienced by the buoy. These simulations were also helpful in determining the specific dimensions of the parts within the WEC sub-system, to translate the heave forces experienced by the buoy into the consistent permeate flow rate of 1 L/min expected of the PFRO system.

3.5.5 Simplified Numerical Model of the System

For the external buoy dynamics, a simplified numerical analysis of its behavior can be made using dynamic relations of the driving forces:

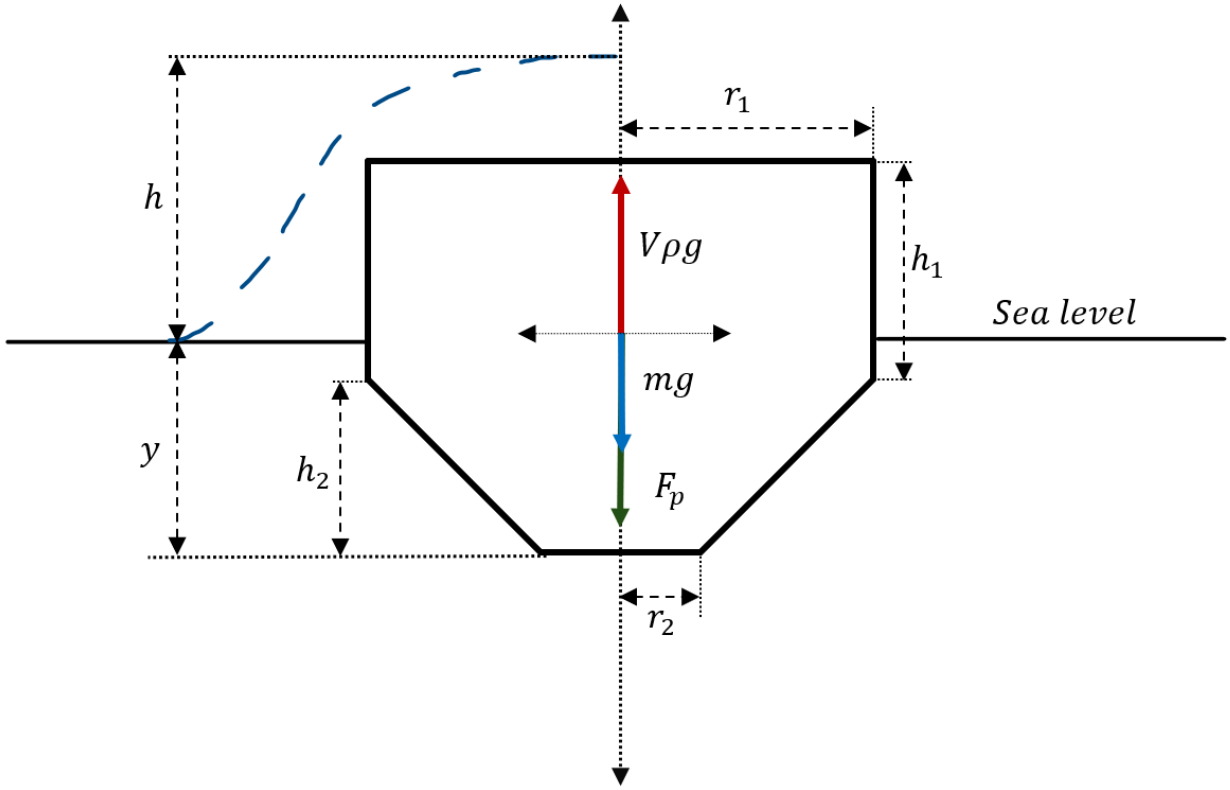

Figure 3.31: Buoy system forces and dynamic relations free body diagram

Here, Vpg refers to buoyancy force, according to Archimedes' principle, as the weight of the displaced volume of water, mg is the buoy's weight, and Fp is the piston's hydrostatic force that the buoy needs to overcome to produce permeate. The dynamics of the buoy are hence dictated by the following equation:

$$\text{Equation 9: } m\frac{d^2y}{dt^2} = V(h - y)\rho g - mg - F_p$$

Given that this is a second-order differential equation, the submerged *y* at equilibrium, and zero initial velocity were taken as initial conditions. It can be noticed that the volume displaced by the buoy is a function of the relative position of the buoy and the wave (*h-y),* and that this function is defined by parts. Numerous assumptions were done to perform this analysis, primarily regarding the wave behavior. The dynamics of the wave, accounted for through the hydrodynamic coefficients file in WEC-Sim, are overlooked, with the assumption that the wave is a plane surface that goes up and down as dictated by the irregular wave pattern obtained from WEC-Sim.

It should be noticed that the system dynamics are not constant over time, i.e. *Fp* behavior changes if the buoy is going up, or down, or if there is not enough force to overcome osmotic pressure. In the case where there is not enough force to produce permeate, the buoy won't be

able to move, so *Fp* would be equal to $V\rho g - mg$, making the acceleration zero, but also the velocity of the buoy must be zero. In the case where the buoy is going down, *Fp* is zero due to the ratchet mechanism. Lastly, when the force exerted by the wave is enough to produce permeate, *Fp* would be a function that depends on the instantaneous osmotic pressure in the membrane and on the position of the piston.

Following the calculations of the crank arm torque, it can be calculated the force felt by the buoy due to permeate production (*Fp*).

$$\text{Equation 10: } \tau = rPA\left(sin\theta + cos\theta \frac{\frac{r}{l}sin\theta}{\sqrt{1-\left(\frac{r}{l}sin\theta\right)^2}}\right)$$

Where τ is the torque of the crank arm, P is the pressure that the piston has to overcome and A is the area of the piston. To get *Fp* from this result, it is assumed a reduction ratio and a radius of the first gear/pinion connected to the rack.

$$\text{Equation 11: } F_p = rPA\left(sin\theta + cos\theta \frac{\frac{r}{l}sin\theta}{\sqrt{1-\left(\frac{r}{l}sin\theta\right)^2}}\right) * \frac{reduction}{r_{gear}}$$

The numerical simulation was made using MatLab. Due to the variable nature of the differential equation depending on the actual circumstances of the buoy, a particular method was used where the code would solve the equation using ode45 during a time span of 0.001s, and then it evaluates the conditions of the buoy movement to decide what *Fp* to use in the next iteration. This process repeated itself until it completed the full 85s time span. The vertical displacement of the buoy was then translated to the angular displacement of the crank arm assembly, resulting in the displacement of the piston from its housing. The calculated values from the piston displacement were used as a basis to perform the irregular wave testing of the PFRO process. The results from this simulation are shown below:

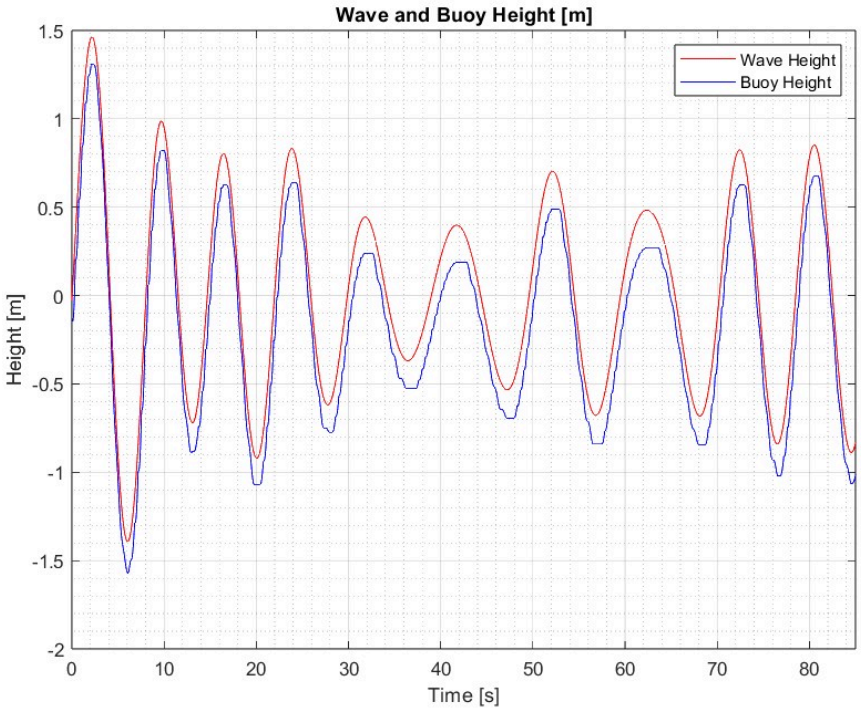

Figure 3.32: Wave and buoy vertical position. Buoy position is referred to the bottom. Wave profile is taken from WECSim

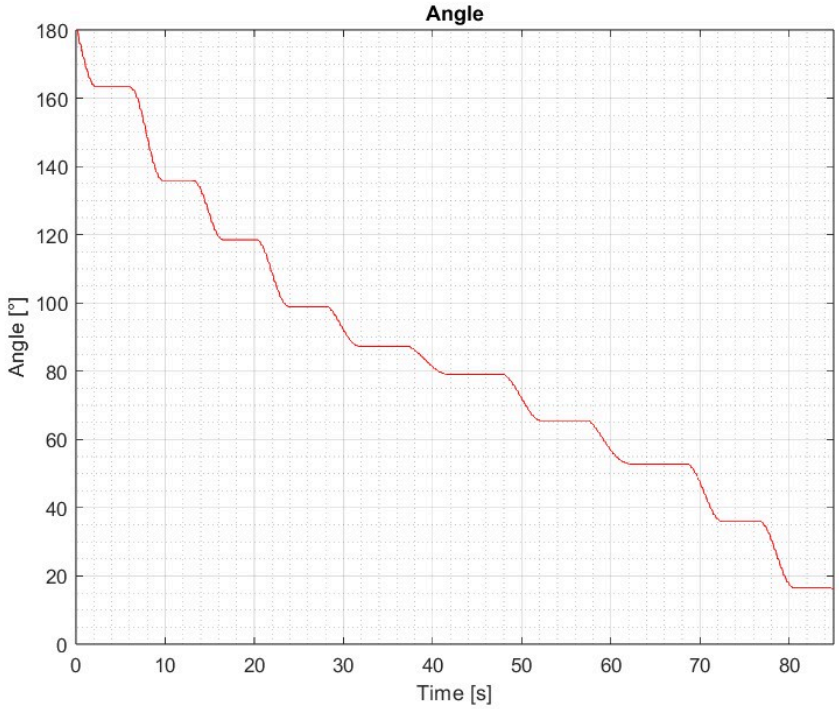

Figure 3.33: Angle of the crank arm mechanism. Initial position is set as 180°.

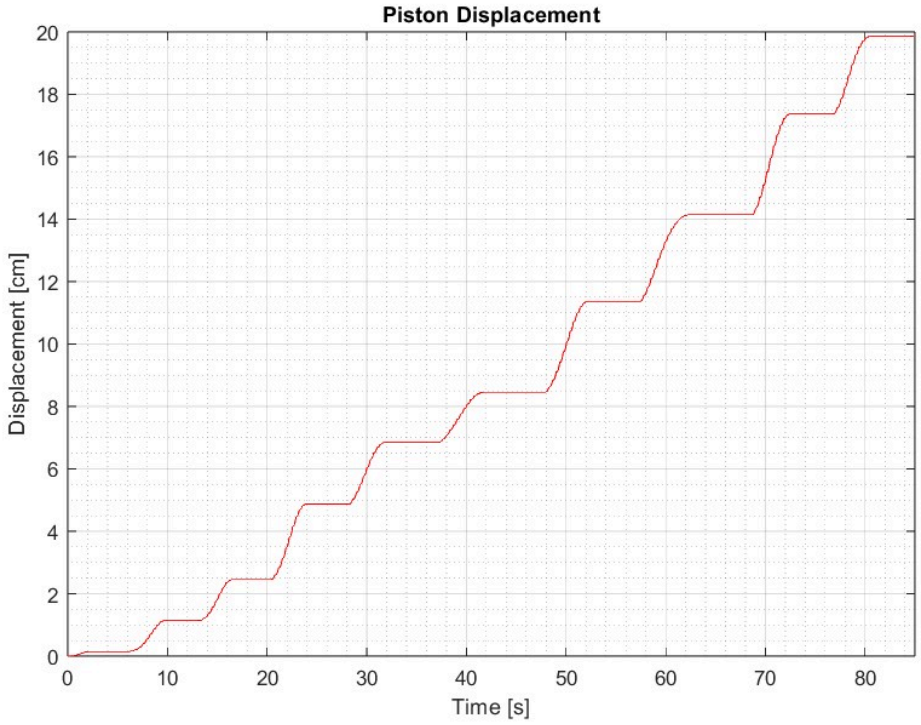

Figure 3.34: Piston displacement over time.

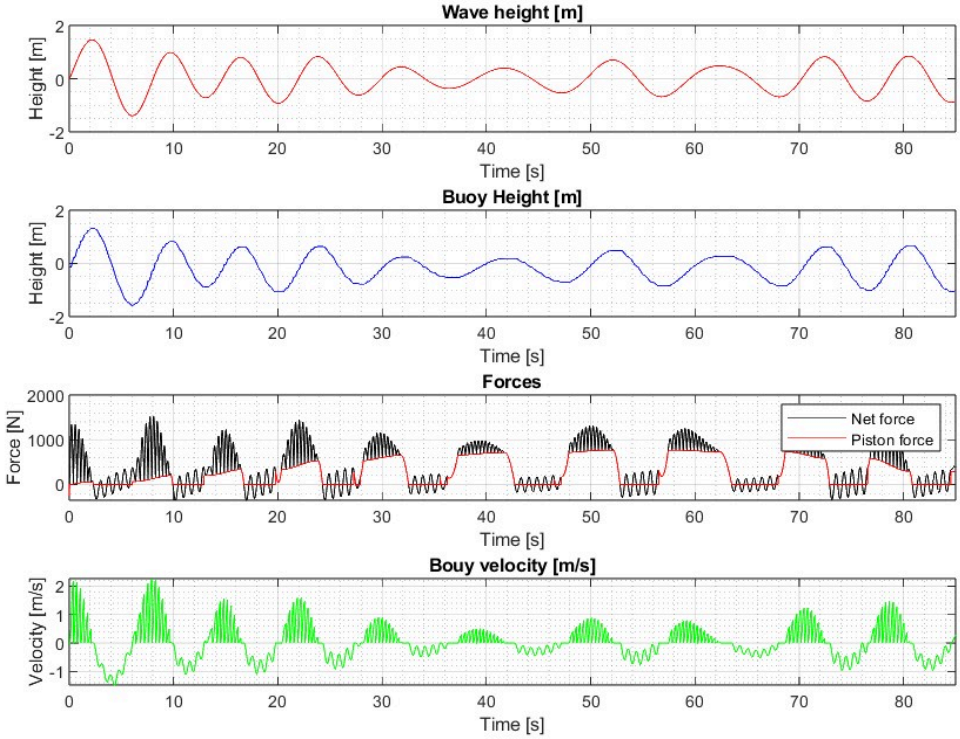

Figure 3.35: Position, forces and velocity of the buoy over time. In the force graph, Net force refers to the buoyancy force minus the weight, and Piston force refers to *Fp*.

From the piston displacement results, it can be observed the pulsed behavior in the permeate production due to the wave pattern. According to this, it went from initial position (0 cm) to 20 cm in a time span of 80 seconds. Supposing these 80 seconds are a representative average wave pattern in the zone studied, and knowing that the area of the piston is 0.0044m^2, there was 0.00088m^3 of water that went to the feed of the membrane, which means 0.66 L/min. Supposing a common recovery ratio of a one-stage RO system of 50%, a 0.33 L/min permeate production would be expected during the permeate phase. From the crank arm angle figure it can be noted that a complete permeate cycle is completed in almost 90 seconds. Since at this time the angle almost reaches 0°.

3.6 System Optimization Efforts

Methods of system optimization were incorporated into all aspects and phases of the engineering design process, from coming up with a novel water filtration device, to the sourcing of the parts in creating a PFRO testbench.

In the team's final design, to ensure fresh water will be available anytime, a fresh water collection tank will be implemented inside the buoy. Therefore, the wave powered desalination device can continue creating and storing fresh water if people decide not to actively use it. Next, the system will have a modular design. Because all the components are connected through threads, the modular design allows for easy removal and installation in case a component fails.

The use of PFRO also upholds the aim of system optimization, as PFRO reduces the risk of membrane fouling due to the repeated fluctuations of hydrostatic pressures, and reduces the need for regular maintenance, other than flipping the reverse osmosis membrane every two years. These design decisions were taken to ensure the priority of the team's device to act as a reliable disaster relief measure, providing water as a main resource to the residents of San Juan, Puerto Rico, rather than being a burden. The emphasis on this aim is also reflected in the team's creation of a passive, purely mechanical PFRO design.

When designing the PFRO testbench at Purdue, the team deliberately invested a lot of time and effort into sourcing quality components to ensure longevity in an ideal scenario. Every component was rated to 65 bar of pressure and is made of stainless steel, to minimize the risk of corrosion to seawater. The team also referred to SAE standards in hydraulic assembly to ensure optimized placement of hoses and other sensitive components, while maintaining a separation of the system's electronics and the hydraulics.

3.7 Environmental and Sustainability Factors

Given the desalination device will be physically anchored to the seafloor, it is crucial for this technology to minimize its environmental impact. Beginning with the intake system, a mesh

filter will be installed to ensure no foreign objects such as fish or seaweed will get trapped in the desalination system. Regarding the brine output, most desalination plants return brine back into the ocean. However, because brine is denser than seawater, it will naturally sink to the seafloor and damage the ecosystem. To solve this, the device will utilize the same solution desalination plants use to safely return brine into the ocean by mixing the brine with seawater, thus diluting the output and avoiding pockets of high salinity brine.

With these solutions in mind, it is still important to realize that a buoy in the ocean will impact the surrounding environment. For example, the movement of the rope through the rising and falling of waves could tangle and interfere with marine life. Therefore, prevention should always be the first option and the locations of buoys should be carefully researched that would have the least environmental impact.

3.8 User Needs

The team's understanding of user needs has been crucial in the engineering design process. After Hurricane Maria, a third of the population of Puerto Rico did not have access to clean water. To combat this, PEARL JAAMS has created a disaster-relief water filtration device.

To ensure that the user can have access to fresh water, water retrieval is explored. In order to get fresh water to land, permeate must be pressurized. Once the permeate is piped to land, a hand pump will be available for people to extract fresh water. Additionally, a pressure exchanger can be installed between the brine and permeate output to further pressurize the permeate, transferring more energy in the permeate to transport it to the shore.

4 Build and Test

4.1 Testbench Design

The team had a few constraints when brainstorming for the MECC competition, such as the lack of access to a wave pool as well as Indiana being a landlocked state. These constraints have made validating the novel design challenging, resulting in the team focusing on validating the PFRO process rather than creating the buoy and the WEC depicted in Figure 3.2. After completing the build, the objective of the experiment was to determine pressure, flow rate, recovery ratio, and power input of the PFRO process.

4.1.1 Mechanical Design

In order to prove the validity of the purely mechanical design, the team designed the test schematic below in Figure 4.1. Here, the 3/2-way valve has three ports and two positions. Additionally, the 2/2-way valve has two ports and two states (open and closed). A pressure sensor is placed before and after the piston to record the system's pressure and ensure it is below the maximum system pressure at those two points. Furthermore, a pressure relief valve is placed

as a regulator to bleed off excess pressure and keep the system under the maximum pressure. Next, flow meters are installed at the location right before entering the RO membrane as well as at the brine output. That way, not only can the feed flow rate be determined but also the brine flow rate and permeate flow rate. The permeate flow rate is the brine flow rate subtracted from feed flow rate. Lastly, the salinity sensors are placed in the brine and permeate tank to track salinity over time.

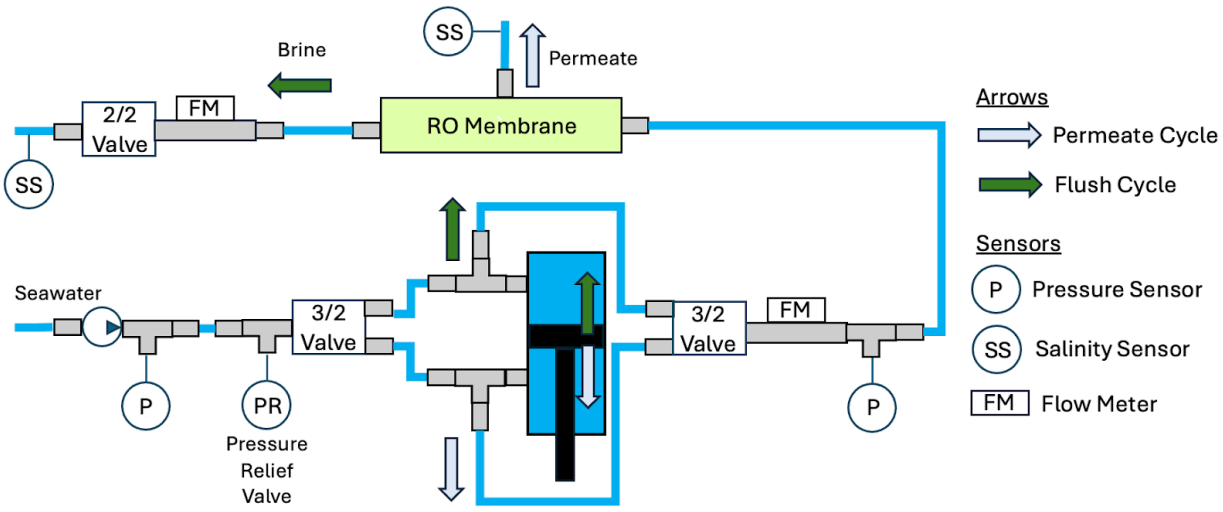

Figure 4.1: System diagram with phase indicators

Beginning with the bottom left, salt water is fed to the pump to be pressurized. First, a pressure sensor determines the pressure of the salt water. Following that, the pressurized salt water connects to a pressure relief valve, set at 750 psi. This relief valve is placed at the beginning of the system so it protects the rest of the components from experiencing high pressures further down the line. Pressurized sea water then enters the 3/2 valve which is directed to either the port that enters into the bore side of the piston or the ports that enter into the rod side of the piston, determining whether the cycle is in the permeate or flushing phase.

During the permeate phase, pressurized salt water from the pump enters the bore side of the piston, causing it to extend. As the piston extends, salt water contained in the rod side of the piston is pushed out and enters the second 3/2 valve, directing the flow to a flow meter, which tracks the feed flow rate, and the feed pressure is measured by another pressure sensor. Salt water then enters the RO membrane. Because the system is in the permeate phase, the 2/2 valve is set to the closed position, blocking the brine output. As a result, all the salt water that has come out of the rod side of the piston is forced to filter through the RO membrane and produce fresh water.

When switching to the flushing phase, all the positions of the 3/2 and 2/2 valves get switched. Rather than pressurized salt water entering the bore side of the piston, the switched 3/2 valve forces salt water to enter the rod side instead, causing the piston to retract. As the piston retracts,

salt water contained in the bore side of the piston is pushed out and enters the second 3/2 valve, directing the flow to a flow meter, which tracks the feed flow rate, as well as another pressure sensor. Salt water then enters the RO membrane. Because the system is in the flushing phase, the 2/2 valve is set to the open position, allowing brine to flow. As a result, the previously supersaturated salt water contained in the membrane during the permeate cycle gets flushed out. The system then switches all the positions of the 3/2 and 2/2 valves, reverting back into the permeate phase.

A CAD model, shown by Figure 4.2 was developed to optimize every location of the components and ensure their dimensions do not conflict.

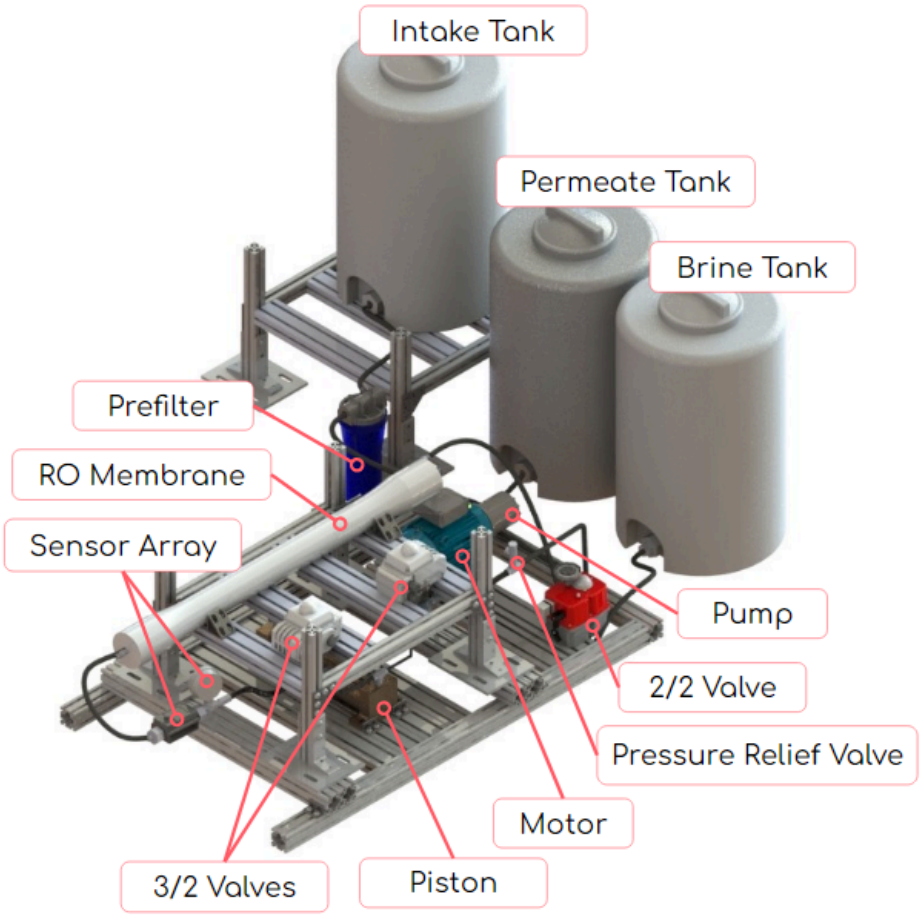

Figure 4.2: CAD model of final PFRO system

There is also a pre-filter installed before the water enters the pump. This ensures that larger particles such as dust in the air can be caught before it enters and damages the pump. Another aspect to note is that the intake tank is placed on an elevated surface to add more hydrostatic pressure, assisting the initial flow into the pump.

4.1.2 Electrical Design

Like mentioned above, due to budget and time constraints, the crankshaft that would originally by actuating the piston back and forth was unable to be manufactured. Instead, the team pivoted to using an electric pump to hydraulically actuate the piston. Despite utilizing electricity to move the piston, the application of the novelty of PFRO can still be validated as the salt water is still going to its exact path as if the system was entirely mechanical.

Next, numerous sensors were implemented in the system to track data using a data acquisition system and validate the PFRO process. Figures 4.3 and 4.4 display the wiring diagrams for the electronics used. Furthermore, the microcontroller was changed from an Arduino UNO to a National Instruments MyRIO, given its more robust hardware and software to perform multiple essential operations simultaneously.

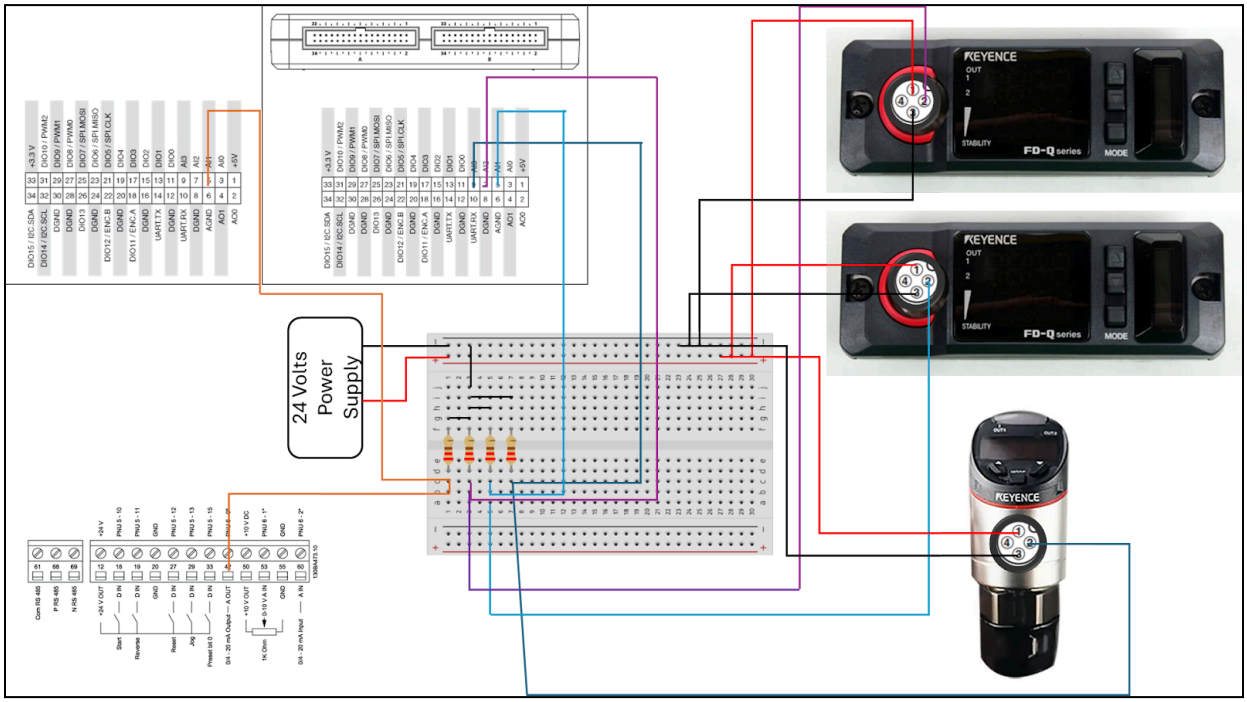

Figure 4.3: Wiring diagram for the system's flowmeters, pressure sensor and VFD output

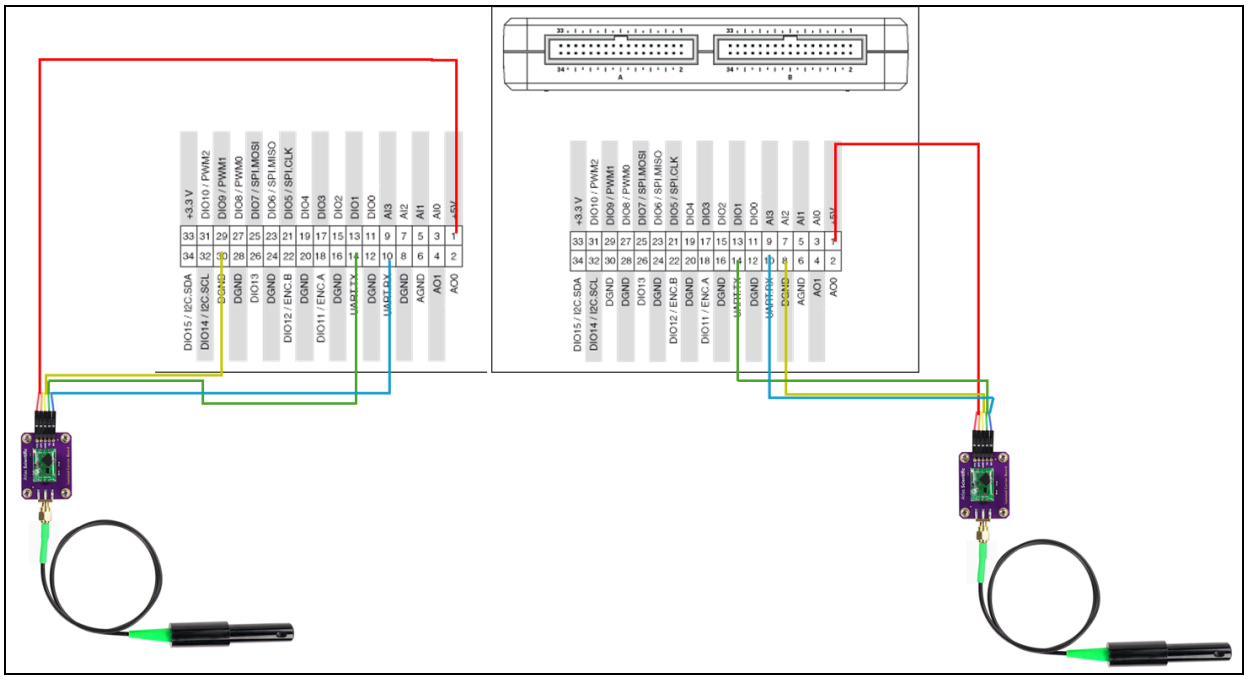

Figure 4.4: Wiring diagram for the system's brine and permeate salinity sensors

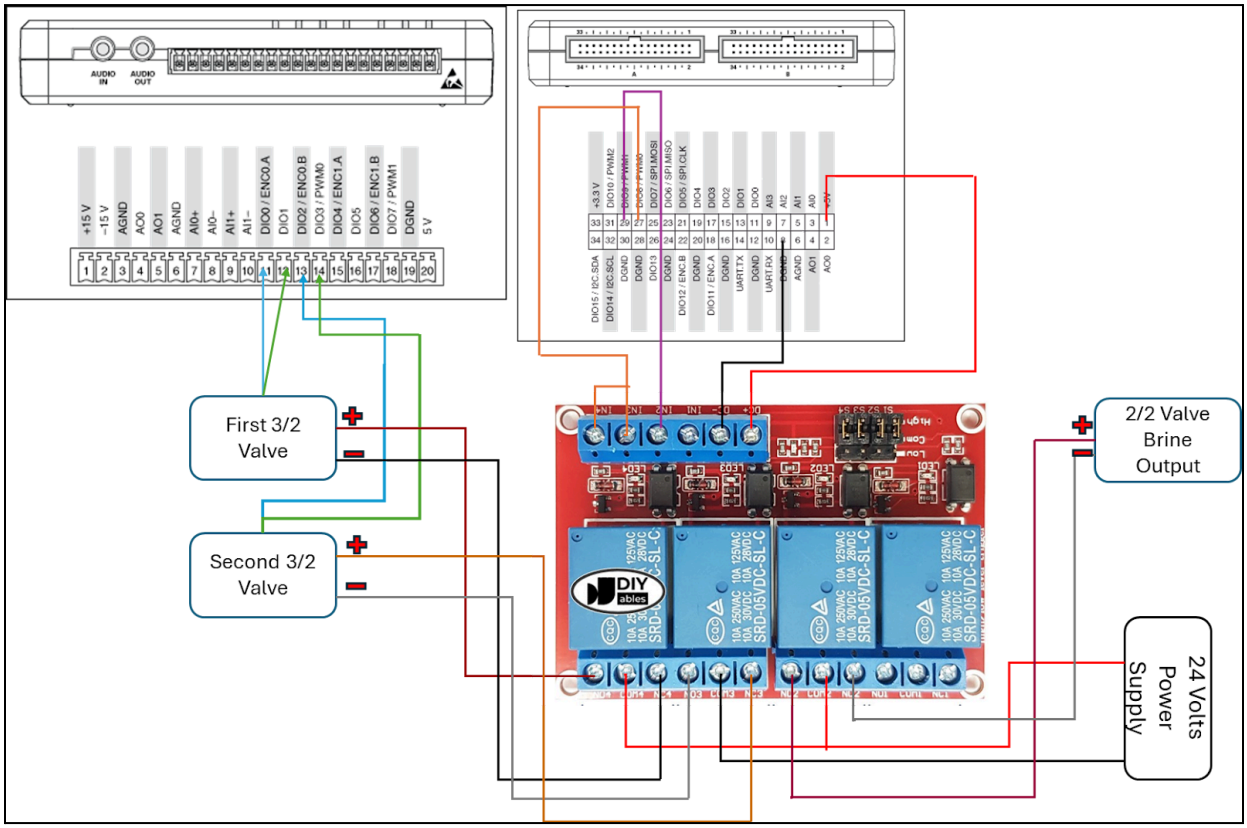

Figure 4.5: Wiring diagram for control of the 3/2 and 2/2 valves and data acquisition for the valve states

The data that were acquired from the experiments through the electronics assembly were:

- Feed Flow Rate (L/min)
- Brine Flow Rate (L/min)
- System Pressure (psi)
- Open/Close Signals of 3/2 valves
- VFD Input Power (kW)
- Brine Salinity (g/L)
- Permeate Salinity (g/L)

The variables controlled through the LabVIEW program were:

- State of 3/2 Valves
- State of 2/2 Valve

The sensors used for data acquisition were two flowmeters (KEYENCE FD-Q20C), a pressure sensor (KEYENCE GP-M100), and two salinity sensors (AtlasScientific EZO-EC). Calibration was required to translate the analog outputs from the flowmeters and the pressure sensor and for the salinity sensors to accurately read the salinity of the brine and permeate outputs in the LabVIEW block diagram. Additional settings were enabled on the VFD to capture the power consumption in the PFRO cycles through its analog output port.

Resistors of 220 Ω were used to translate the analog current outputs (ranging from 4mA to 20mA for the flowmeters, pressure sensor, and the VFD output) to analog voltages to be captured by the MyRIO through its analog input ports. The Universal Synchronous Receiver-Transmitter (UART) ports on the MyRIO were used to record the salinity levels from the sensors. The sensors were connected to their power supply block.

The control of the 3/2 and the 2/2 valves, as mentioned, was incorporated in the MyRIO through LabVIEW. The operation of the PFRO cycle requires the operation of the 3/2 valves to be synchronized, wherein the permeate phase, the first 3/2 valve and the 2/2 valve are closed while the second 3/2 valve is open. In the flushing phase, the first 3/2 valve and the 2/2 valve are open, while the second 3/2 valve is closed. To reflect these operations electronically, a 5V digital four-relay block was used. Additional wiring was done to obtain the open/closed signals from the 3/2 valves, to represent the PFRO phases. The valves were powered by another power supply block. The optimization of wiring required for these operations was done by creating required connections in a soldering board.

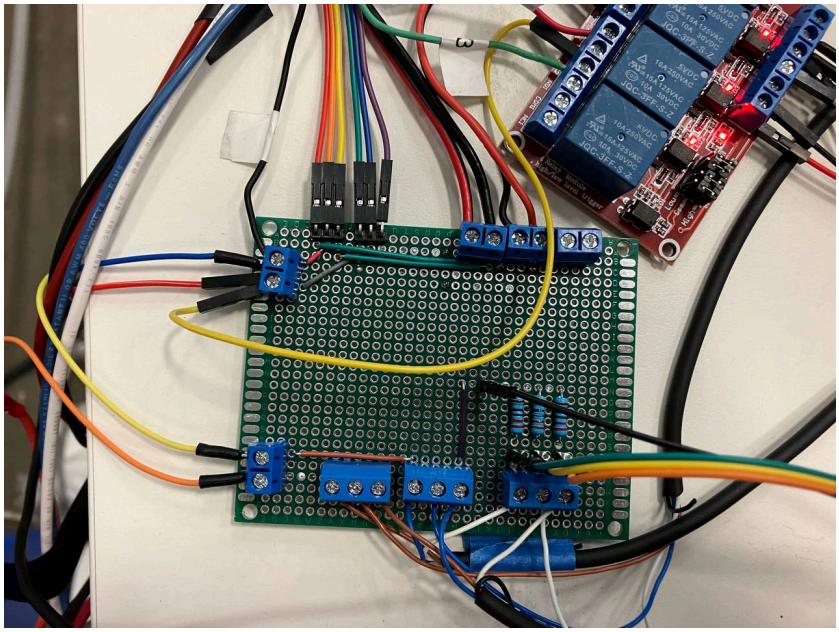

Figure 4.6: Soldered board to optimize electrical connections for valves and sensors

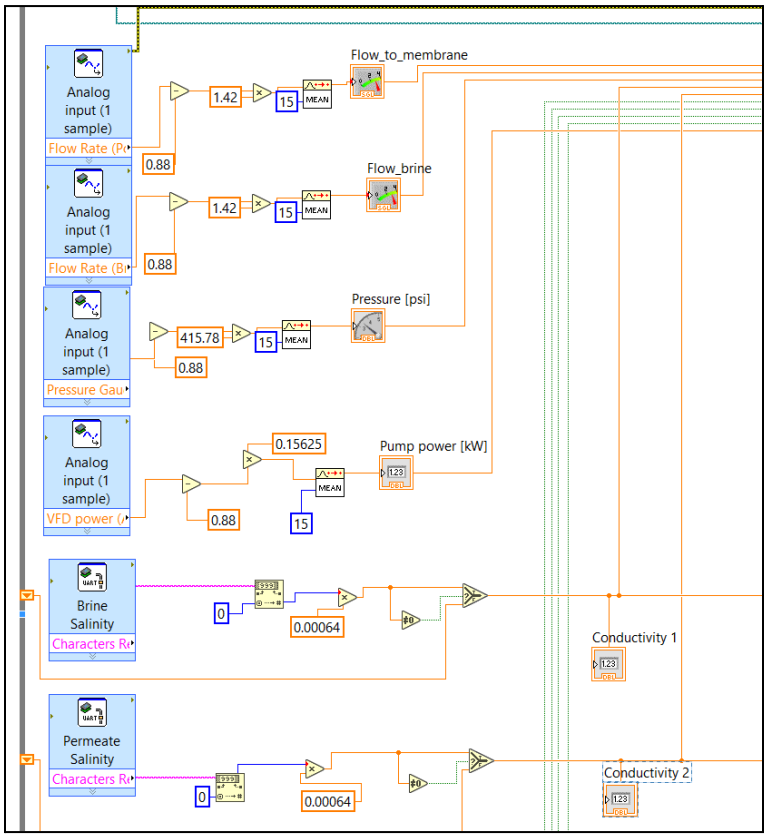

Figure 4.7: Labview block diagram - sensor unit conversion

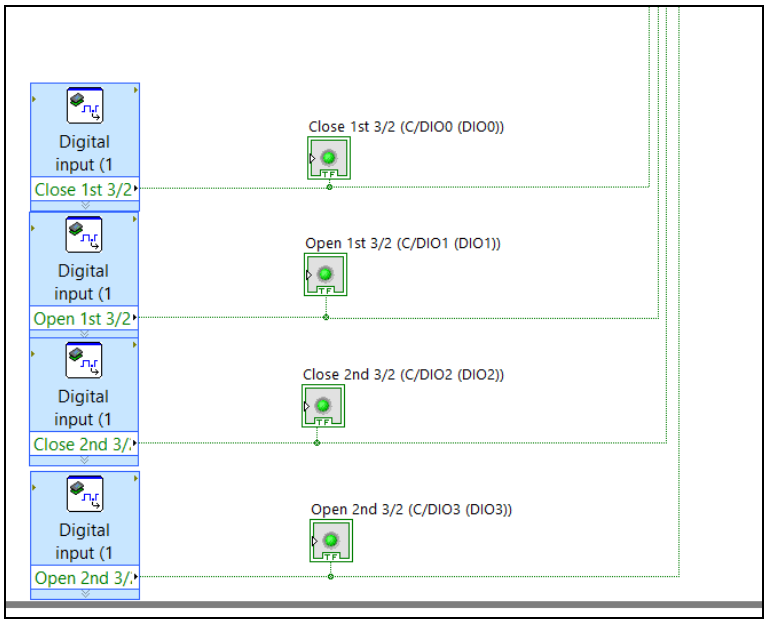

Figure 4.8: Labview block diagram - valve state indicators

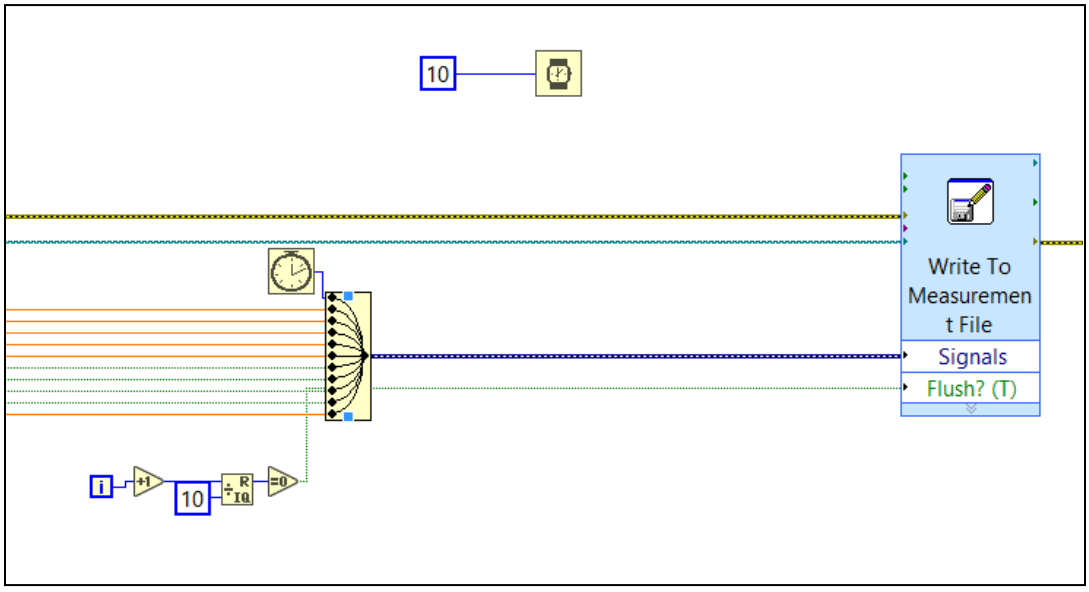

Figure 4.9: Labview block diagram - sensor unit conversion

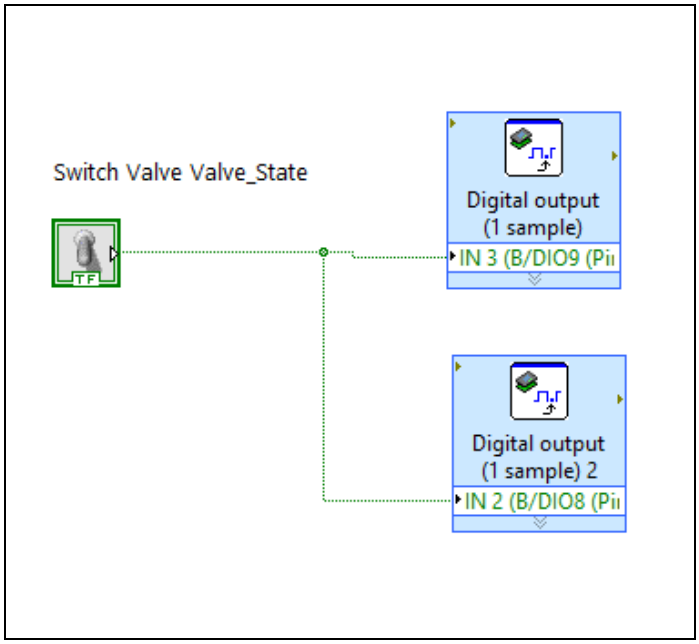

Figure 4.10: Labview block diagram - valve control switch

The LabVIEW block diagram can be seen in Figures 4.7-4.10. Data is captured every 100ms, with an average of 15 values captured for the flow meters, the pressure sensor, and the VFD power output. The inputs from the salinity sensors are captured in a similar way. As depicted in the figures, the first six inputs are adjusted with calculations to convert analog voltages to the appropriate unit and reading. Likewise, the binary values of the open/close signals of the 3/2 and the 2/2 valves are recorded. Then, all these signals, with a timer, were attached to a *Write to Measurement File*, stored as an Excel file on the MyRIO. The control of the three valves were incorporated as a switch on the block diagram, outputting to two digital outputs that are passed to the actuating relay blocks.

Figure 4.11: Labview front panel control

The LabVIEW front panel can be seen in Figure 4.11. Beginning with the top left, there is a box that allows the user to rename the excel file during data exporting. Moving towards the middle, there is a pressure sensor, flow meters for feed and brine, salinity sensors for permeate and brine, and finally valve switches for whether the system is in the permeate or flushing phase. Lastly, the switch on the right flips both the 3/2 valves and the 2/2 valve, cycling between the permeate and flushing phase.

4.2 Physical System

4.2.1 Initial Device Assembly

The final design changed in multiple critical ways during the last few weeks of its construction to become fully realizable within the given timeline and scope. Due to a combination of part delays, budget constraints, and an updated testing timeline, there was a change in the focus of the crankshaft design. A motor and pump would instead be used to simulate the wave motion; actuating the piston by gradually pressurizing opposite chambers, instead of displacing the piston arm. Thus, the team's new goal was to electronically and physically validate that a PFRO system could be constructed, and to simulate the ideal, fully mechanical design.

Although the final design within the buoy will be made light in order to efficiently capture the wave energy, the team's PFRO validation device will be primarily focusing on testing functionality rather than final buoy integration. This meant aluminum 80/20 beams were chosen as the primary structural component, as they offered high levels of adjustability even while being heavy for the final buoy system.

The first prototype of the team's final design began with laying an 80/20 base using two long beams parallel to one another and slotting in four shorter beams between those. This creates a solid rectangular base with two cross beams to attach components.

4.2.2 Assembly Process Plan

The team then created a process plan to describe each step in assembly of the final device design. This can be seen in the following tables.

Table 4.1: Membrane Assembly Process Plan

Step	Description
1	Secure piston and motor to 80/20 structure
2	Connect driving arm to motor
3	Connect 1/2" M NPT to 1/4" M NPT fitting to both piston ports
4	Connect 1/4" F NPT T connector to both of the prior fittings
5	Set membrane housing on 80/20 structure
6	Secure membrane housing to 80/20 structure in correct position
7	Connect 1/4" NPT M to 1/4" NPT M fitting to all 3 membrane ports
8	Connect permeate port to permeate tank with hose
9	Connect intake port of membrane to 1/4" M NPT to hose fitting with hose
10	Connect brine port to 1/4" F NPT actuating ball valve with hose
11	Connect one outlet of the ball valve to brine tank with hose
12	Connect the other ball valve outlet to a 1/4" NPT M to 1/4" NPT M fitting
13	Connect that fitting to a 1/4" F NPT T connector
15	Connect the T connector to a 1/4" F NPT swivel to hose fitting
16	Add a pressure relief valve to the T connector
17	Connect the pilot line to one end of the T connector

Table 4.2: Piping Process Plan

Step	Description
1	Connect the open end of the pre-filter to 1/2" M BSPP to 1/4" F NPT
2	Connect a 1/4" M NPT to 1/4" M NPT fitting
3	Connect a 1/4" F NPT swivel that connects to a hose
4	Connect a 1/4" M NPT to hose fitting at the end of the hose
5	Connect a 1/4" F NPT T connector

6	On one end of the T, connect a 1/4" M NPT to a length of hose
7	Connect that hose to the piston's flushing port using a 1/4" F NPT swivel
8	Add a check valve between the fitting and the piston port
9	The other end of the T connects to the piston's permeate port with a check valve
10	Building off from the other T connector at the piston's permeate port, add a check valve
11	Connect the check valve to yet another T connector
12	Use a hose with F swivel fittings to connect one end of the permeate T to flushing T connector
13	Add a check valve between the hose and the flushing T connector
14	Secure the pilot line from the membrane subsystem to the same T connector
15	On the other end of the permeate T connector, connect a 1/4" M NPT to 3/4" F NPT fitting
16	Connect a 1/4" M NPT to 3/4" F NPT fitting
17	Connect that fitting to a 6" stainless steel pipe
18	Attach a flow meter to the pipe
19	Connect the pipe to a 1/4" M NPT to 3/4" F NPT fitting
20	Connect a 1/4" F NPT T connector
21	Connect a 1/4" M NPT to hose fitting
22	Connect a line of rubber hosing to the end of that fitting
23	Use a 1/4" F NPT swivel to connect the hose to the membrane intake
24	Connect a pressure relief valve to the first T connector mentioned
25	Connect a pressure gage to the second T connector mentioned

Table 4.3: Support and tank assembly process plan

Step	Description
1	Set out three tanks (intake, brine, and permeate) at the side of the structure
2	Connect each tank input to 3/4" F NPT to 3/4" F NPT fitting
3	Then connect that fitting to 3/4" M NPT to 1/2" M NPT fitting
4	Then connect that fitting to 1/2" F NPT to 1/2" F NPT fitting (quick release)
5	Connect 1/2" M rubber hose for quick release to fitting
6	Connect 1/2" F NPT (quick release) to 1/2" M NPT fitting to end of feed tank hose
7	Connect pre-filter to previous fitting for feed tank hose
8	Connect 1/2" M NPT to 1/2" F NPT (quick release) fitting to other end of pre-filter
9	Secure pre-filter to 80/20 supports with aluminum bands

This process plan resulted in a functional PFRO validation device with simulated wave energy power using the motorized piston.

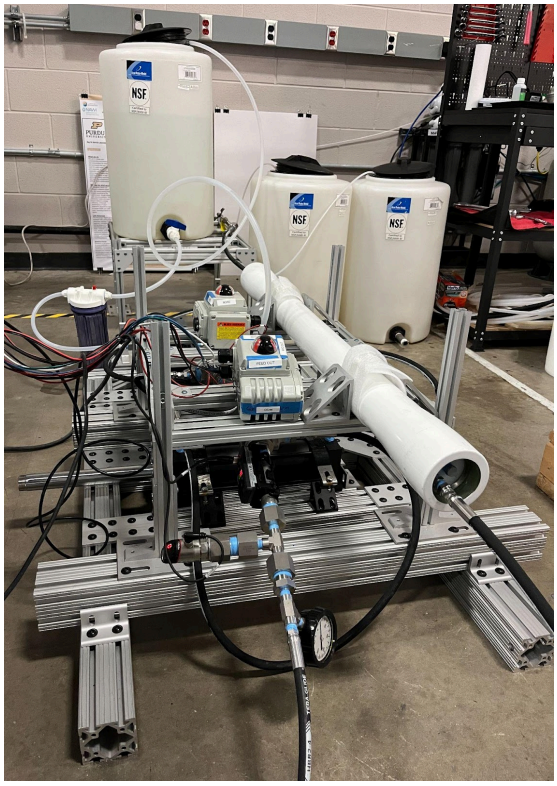

Figure 4.12: Side view of final prototype

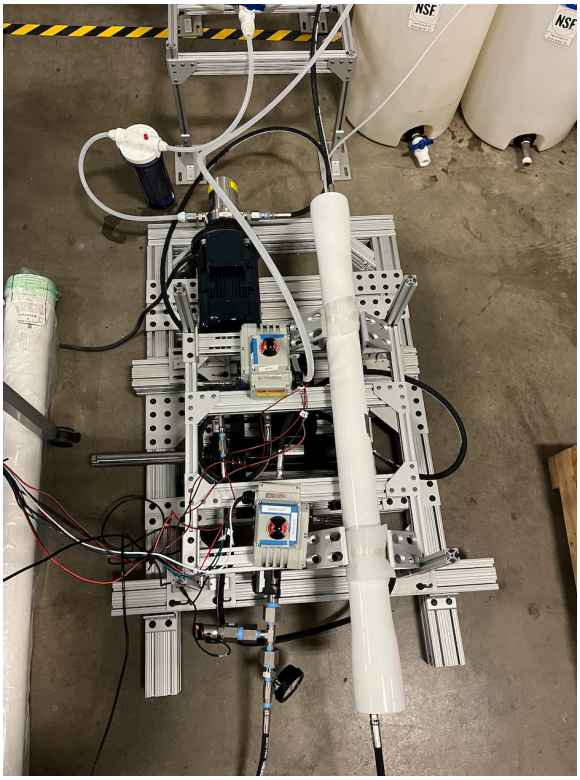

Figure 4.13: Top view of final prototype

Figure 4.14: Internal view of final prototype with piston extended

4.3 Design Iterations

As testing and validation matured, there were additional shifts in placement, materials used and subsystem structure as more efficient methods became clear. A separate 80/20 structure to elevate the membrane housing and 3/2 valves above the pump, motor, and piston, and to prevent pipe kinks. As a consequence of eliminating the crankshaft, the piston position had to shift to be perpendicular to the membrane housing and fit between the two supporting 80/20 beams on the lower level of the structure. The feed tank also had to be lifted on its own 80/20 support structure in order to allow gravity to assist the initial flow into the pump. The prefilter was also removed from this portion of the prototype because it caused several leaks and was deemed not necessary enough to consistently manage. On the far side of the system, a 2/2 valve was put in as the brine blocking system to replace the pilot-operated ball valve.

In addition to mechanical changes, the design of the electronics assembly has been updated to electronically activate the new 3/2 and 2/2 valves, grounded in creating systems of data acquisition and control of 3/2 valves. Simulation using wave data using a microcontroller was not conducted due to constraints in the overall PFRO system, such as the pump used and the actuation of the pressure relief valve. Quantifying the input and the output flow rates of the piston is essential in simulating the wave motion, and the pump's flow rate was too high and the actuation of the pressure relief valve led to a reduction of control between the prescribed flow rate and the actual feed flow rate.

The electronics had to be shifted in order to fall outside the possible path of leaking valves. Another safety concern was the unknown pressure pre-pump. To mitigate this, the team added an analog pressure sensor right before the pump. This aids the team in two ways: it helps to verify the digital pressure sensors are functioning correctly, and adds another level of security in that it ensures the pump does not experience damage from highly pressured water.

4.4 Testing Process

After successfully creating the PFRO device, 5 tests were run to ensure the system's safe and smooth operation. These tests were pressure sensor calibration, pressure relief valve calibration, flow meter calibration, salinity sensor calibration, and pressure test. Two levels of calibration were required for the pressure sensor and the flowmeters, as the readings displayed on the Keyence sensors had to be cross-checked against analog sensors or calculations, and the second form of calibration was done to ensure that the analog current output detected by the NI MyRIO was similar to the value displayed on the sensor.

Note that the brine output that originally had the 2/2 valve is replaced with a flow adjustment valve for manual tuning. Additionally, VFD (variable frequency drive) controls the flow rate of the pump by controlling the power transferred from the 3-phase AC power supply to the 3-phase motor that powered the positive displacement pump. A positive displacement pump was used to

maintain a consistent flow rate regardless of the system pressure. The procedures of the different tests can be found below:

Pressure Sensor Calibration

1. Set VFD to 5 Hz
2. Increase pressure by increments of 100 psi by slowly closing the flow adjustment valve
3. Confirm readings of pressure sensor with manual pressure gauge and adjust pressure sensor accordingly

Pressure Relief Valve Calibration

1. Set VFD to 5 Hz
2. Increase pressure by slowly closing adjustment valve until 740 psi is reached
3. If pressure relief valve is not activated when 740 psi is reached, turn off pump and adjust pressure relief valve spring (tighten/loosen) until it activates at 740 psi

Flow Meter Calibration

1. Set VFD to a frequency until 1 L/min is reached
2. Open adjustment valve fully and allow flow to collect in bucket for 1 minute
3. Compare volume of water collected with 1 L and adjust flow meter accordingly

Salinity Sensor Calibration

1. Measure out 105 g of salt and mix with 3 L of water (35 g/L, seawater salinity)
2. Compare solution salinity with salinity sensor and adjust accordingly

Pressure Test

1. Set the VFD to 0 Hz
2. Use laptop and data acquisition system to begin data collection process (pressure and flow rate vs time)
3. Slowly increase the frequency of the VFD to match a pressure increase rate of 5 psi per second (10 psi per second maximum) until 1 L/min is reached
4. Slowly close the flow adjustment valve to match a pressure increase rate of 5 psi per second (10 psi per second maximum) until 740 psi is reached
5. IF RELIEF VALVE IS ACTIVATED: Slowly fully close the flow adjustment valve while ensuring the pressure is not increasing and that the pressure relief valve is still activated
6. IF THERE IS A LEAK: Follow the shut-down procedure and re-tape/re-tighten fittings

After calibrating the system's sensors and completing the pressure test, the PFRO system was ready for data collection. To validate the PFRO design as well as determine the experiment's objectives, two main tests were conducted: regular wave motion and irregular wave motion. The first test is an ideal regular wave test in which the piston oscillates back and forth in a perfectly

sinusoidal motion. The reason this test is conducted is to determine how the system performs under ideal conditions. The test procedures are as follows:

Regular Wave PFRO Test

1. Turn on the LabVIEW software to collect data and control the 3/2 valves
2. Turn the setup to permeate cycle mode (direct flow to bore side, close 2/2 valve)
3. Turn the pump to 4 Hz
4. Observe the piston extend and permeate being produced as the pressure increases
5. Once the piston is fully extended, turn off the pump
6. Switch the setup to flushing cycle mode (direct flow to rod side, open 2/2 valve)
7. Turn the pump to 4 Hz
8. Observe the piston retract and the brine being flushed
9. Once the piston is fully retracted, turn off the pump
10. Repeat Step 2-9 three times
11. Turn off the LabVIEW and analyze the data

Next, an irregular wave test was conducted. Wave data was taken from WEC-Sim simulation conducted with an .stl file of the buoy, with parameters such as the significant wave height of 2 meters and average wave period of 8 seconds being taken from buoy data from San Juan, Puerto Rico. Next, through a series of gear reductions, the amplitude of the waves was taken and converted into piston displacement shown by Figure 4.16.

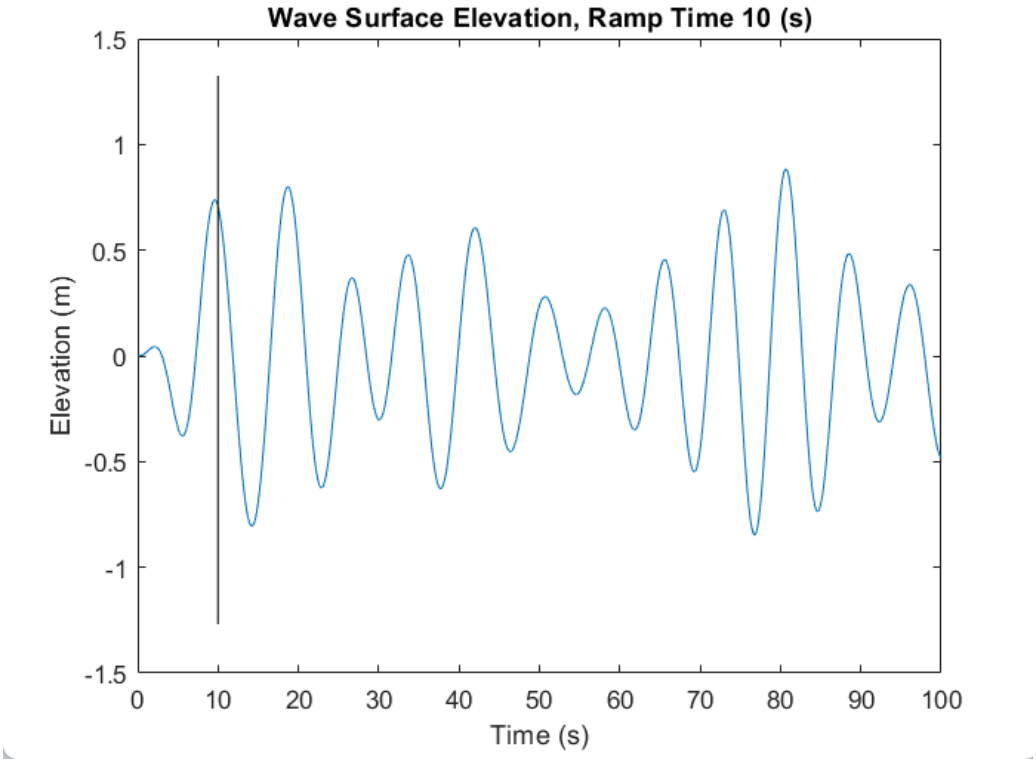

Figure 4.15: Elevation of the wave surface with respect to time (s)

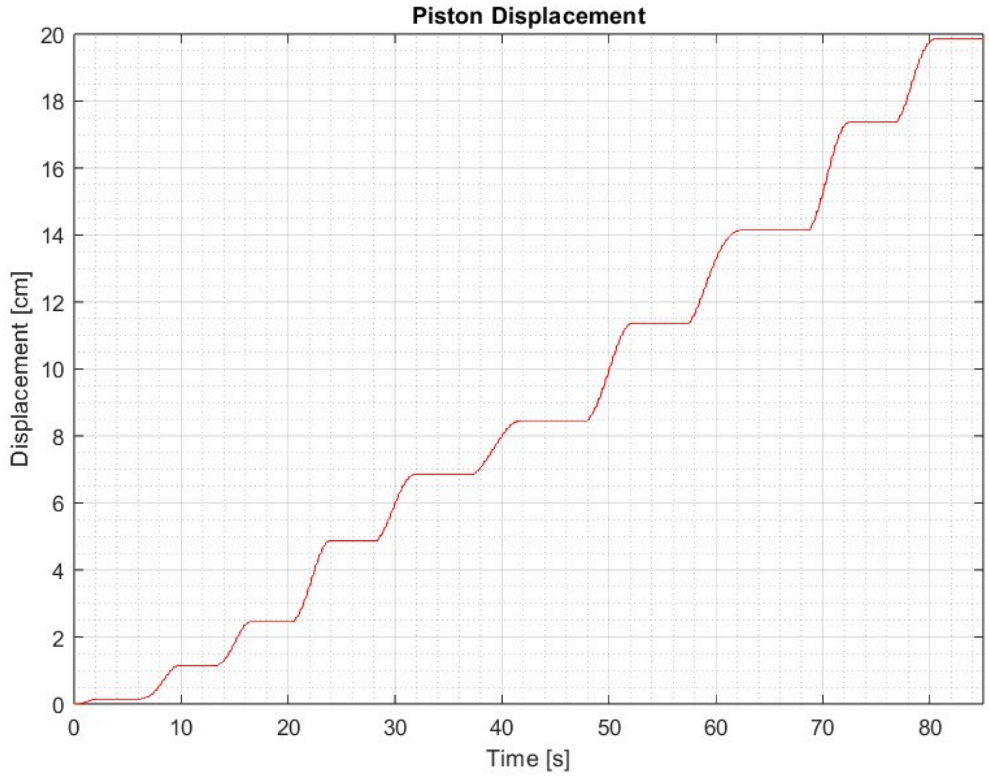

Figure 4.16: Piston displacement with respect to time (s)

Given the now converted data set, the test procedures are as follows:

Irregular Wave PFRO Test

1. Begin LabVIEW data collection
2. Set valves to permeate cycle
3. Set VFD to 5 Hz
4. Observe as the piston extends to marked stopping points on a tape measure and stop for a set time, both derived from irregular wave data
5. Observe as the piston extends and stop the VFD when the piston is fully extended
6. Set valves to flush cycle
7. Set VFD to 5 Hz
8. Repeat steps 4-5 with flush cycle

After performing both tests, the PFRO system was able successfully desalinate seawater and produce fresh water through the movement of a pressurized piston.

Additionally, through both these tests, raw data (time, pressure, flow rate, input power, salinity) is extracted through the sensors. A section of the raw data collected through LabVIEW is seen in Figure 4.17. One section to note is that “Close 1”, “Open 1”, “Close 2”, Open 2” tracks the valve

locations which determines whether the system is in the permeate phase (1 0 0 1) or flushing phase (0 1 1 0).

Time [s]	Feed flow [L/min]	Brine flow [L/min]	Pressure [psi]	Brine salinity [g/L]	Permeate salinity [g/L]	Close 1	Open 1	Close 2	Open 2	Power [kW]
0	-0.041421	-0.095157	10.711169	35.93024	11.1936	1	0	0	1	0.087376
0.312	-0.053555	-0.049222	8.934765	35.93024	11.1936	1	0	0	1	0.10912
0.38	-0.01542	-0.036221	4.620642	35.93024	11.1936	1	0	0	1	0.088012
0.451	0.00408	-0.053122	-0.327911	35.93024	11.2	1	0	0	1	0.092717
0.522	0.018901	-0.044542	-1.571393	35.93024	11.2	1	0	0	1	0.102444
0.593	0.031959	-0.041999	0.644882	35.93024	11.2	1	0	0	1	0.087376
0.665	0.017514	-0.047612	-1.324872	35.93024	11.2	1	0	0	1	0.093289
0.736	0.017731	-0.042288	-2.358086	35.93024	11.2	1	0	0	1	0.086137
0.808	0.019248	-0.039303	-0.849553	35.93024	11.2	1	0	0	1	0.079726
0.879	0.016994	-0.033101	-0.454797	35.93024	11.2	1	0	0	1	0.076886
1.404	0.015781	-0.019202	-1.377604	35.93024	11.1936	1	0	0	1	0.081221
1.836	0.01607	-0.016865	-1.004636	35.92384	11.1936	1	0	0	1	0.079524
1.908	0.012581	-0.014087	-0.923299	35.92384	11.1936	1	0	0	1	0.076416
1.98	0.016276	-0.014925	-0.128519	35.92384	11.1936	1	0	0	1	0.082077
2.05	0.015318	-0.022123	-0.894668	35.92384	11.1936	1	0	0	1	0.078742
2.123	0.019594	-0.017269	-1.199195	35.92384	11.1936	1	0	0	1	0.078628
2.194	0.021328	-0.018887	-2.078937	35.92384	11.1936	1	0	0	1	0.074279
2.265	0.010927	-0.017501	-2.654154	35.92384	11.1936	1	0	0	1	0.079544
2.337	0.000989	-0.004211	-1.436048	35.92384	11.1936	1	0	0	1	0.079849
2.403	-0.001091	0.000758	-1.60523	35.92384	11.1936	1	0	0	1	0.071266
2.885	-0.010914	0.000989	-3.263206	35.93024	11.1936	1	0	0	1	0.074394
3.318	-0.003749	0.006074	-3.432388	35.93024	11.1936	1	0	0	1	0.074228
3.391	-0.000513	0.00018	-4.31213	35.93024	11.1936	1	0	0	1	0.075207
3.462	0.002029	0.000411	-5.868598	35.93024	11.1936	1	0	0	1	0.079175
3.533	0.005496	0.000296	-7.255885	35.93024	11.1936	1	0	0	1	0.081654
3.605	0.00746	-0.005251	-6.30847	35.93024	11.1936	1	0	0	1	0.078361
3.675	0.010812	-0.007216	-6.57916	35.92384	11.1936	1	0	0	1	0.076123
3.747	0.014625	-0.013687	-6.071616	35.92384	11.1936	1	0	0	1	0.075729
3.819	0.013932	-0.011954	-6.951359	35.92384	11.1936	1	0	0	1	0.071647

Figure 4.17: Raw data of time, flow rates, pressure, salinity, valve positions, and input power

The raw data was then analyzed and refined to obtain achievable and readable results. Because the flowmeter sensor is unable to read the flow rate in the reverse direction, negative flow rate values are set to 0. This was done as the flowmeters cannot read flow in both directions and hence cannot detect any backwash. Additionally, the permeate flow rate can be numerically determined by subtracting the feed flow rate from the brine flow rate. The results were then plotted to obtain visual representations of the data obtained from the experiments that the team ran.

Regular Wave Results

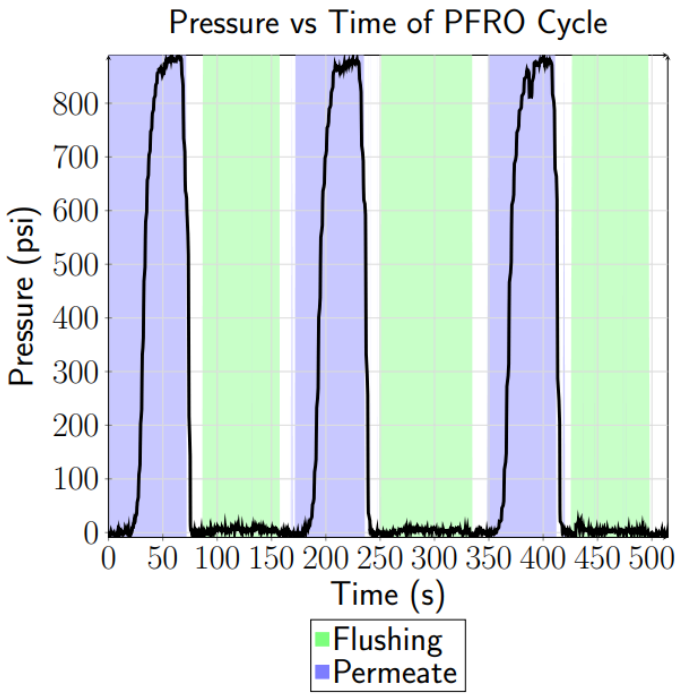

Figure 4.18: Data of system pressure vs. time, with respect to PFRO cycle

As seen in Figure 4.18, it is clear that pressure build-up occurs during the permeate cycle while there is no pressure build-up during the flushing cycle. These results confirm the design goals as there should only be pressure build-up during the permeate phase. The reasoning behind this is that the 2/2 valve blocks the brine output during the permeate cycle, causing the pressure to rise as salinity increases. The maximum pressure is determined to be 890 psi.

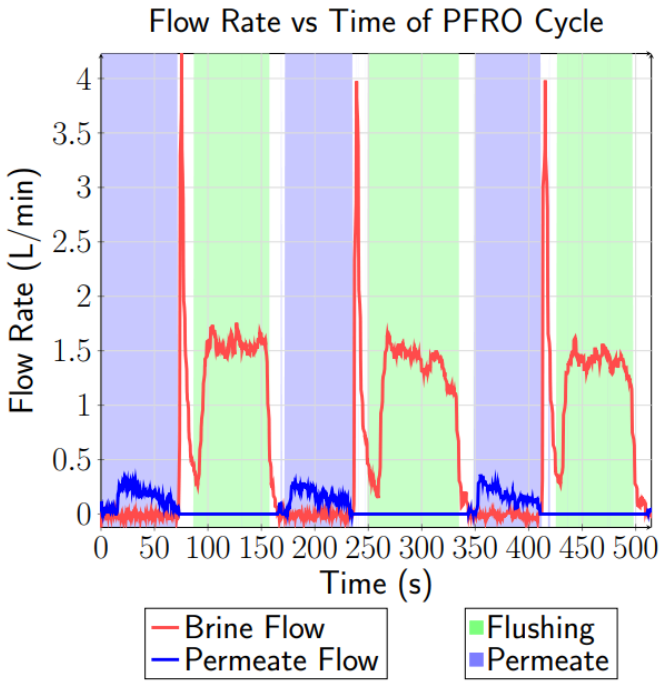

Figure 4.19: Data of fluid flow rate vs. time, with respect to PFRO cycle

As seen in Figure 4.19, the graph depicts the flow rate of the permeate and brine throughout the test. When the system is in the permeate phase, there is permeate production shown by the blue line while there is no brine production due to the brine blocking. However, when the system is in the flushing phase, the brine production is shown by the red line as the brine is getting flushed out. The spikes in the brine production occur during the transition from the permeate to flushing cycle. This is because the large buildup of pressure in the membrane created from the permeate cycle causes a large brine flow once the brine output is opened when the system is transitioning from the permeate to the flushing cycle.

Through this graph, the peak feed flow rate was determined to be 0.439 L/min. Additionally, the recovery ratio can be determined. By integrating both flow rates with respect to time, the total permeate produced and total brine produced, and by dividing the permeate produced by feed input, a recovery ratio of 29% was determined.

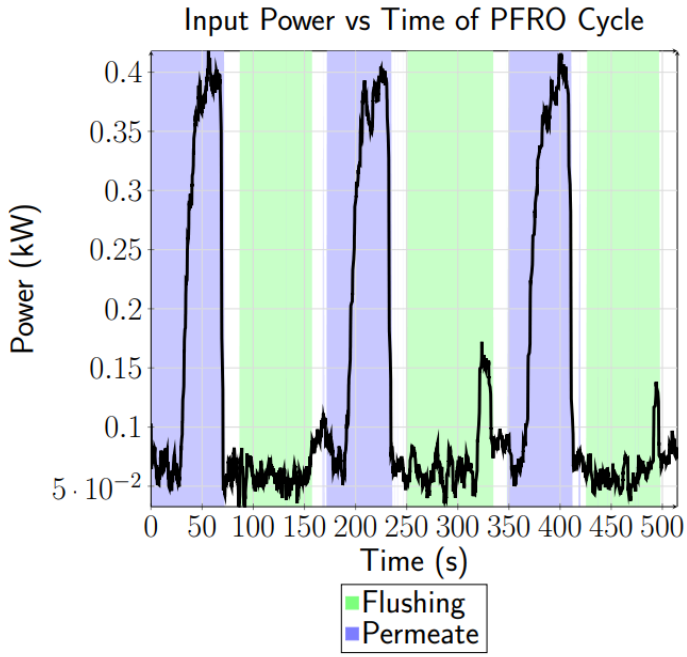

Figure 4.20: Data of input power vs. time, with respect to PFRO cycle

As seen in Figure 4.20, the graph depicts the power consumption measured by the VFD through the test. From this graph, it is clear that the power consumed is significantly higher when the system is in its permeate phase compared to flushing phase. This makes sense as the system needs to reach a higher pressure during its permeate phase compared to flushing phase. Therefore, more energy is required to achieve the higher pressure. By integrating the graph, the total power consumption during the test can be determined. By dividing the power consumption by the total permeate produced, a value of 37.1 kWh/m^3 of permeate is determined from the system. Compared to a value of 4 kWh/m^3 for a typical desalination power plant, these inefficiencies in the system range from the frictional losses from the piping and piston to an oversized motor, running the system at an extremely low rpm and losing efficiency. Additional calculations were done based on the specific energy consumption (SEC) of the feed using Equation 12.

$$\text{Equation 12: } SEC = \frac{\int_0^{t_{end}} PQ_{feed}\,dt}{\int_0^{t_{end}} Q_{permeate}\,dt}$$

Based on this calculation, the energy used was 1.06kWh/m^3.

The predicted and actual valve metrics can be seen in Appendix G. Through this table, although the design does not achieve the desired numerical results, the overall function was successful.

Irregular Wave Results

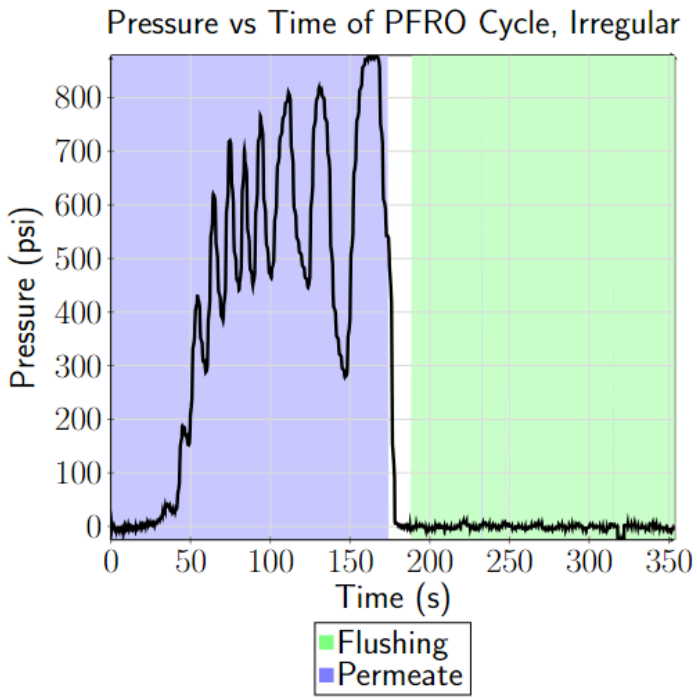

Figure 4.21: Irregular wave data of pressure vs. time, with respect to PFRO cycle

Figure 4.21 depicts the pressure vs time. The spikes in the pressure during the permeate phase reflect the irregularities in the real-world wave data. However, the system still reached a maximum of 890 psi when the piston is fully retracted.

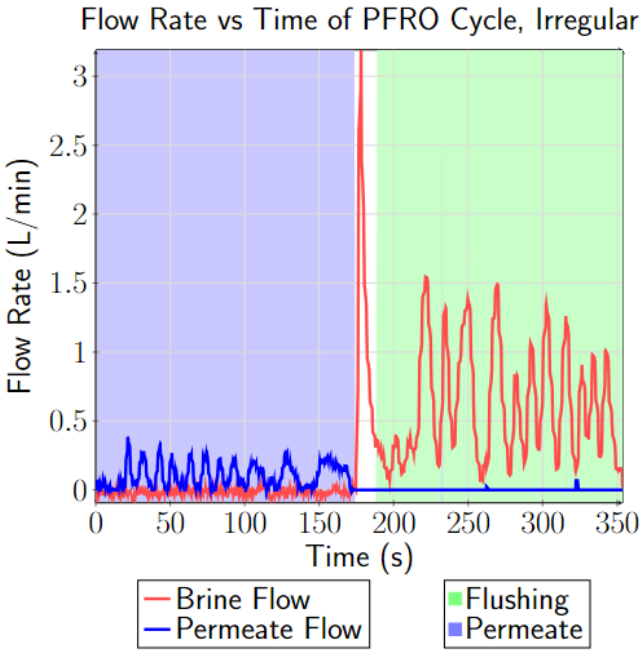

Figure 4.22: Irregular wave data of flow rate vs. time, with respect to PFRO cycle

Figure 4.22 depicts the flow rate vs time. The spikes in the permeate flow during the permeate phase and brine flow during the brine flow also reflect the irregularities in the real-world wave data.

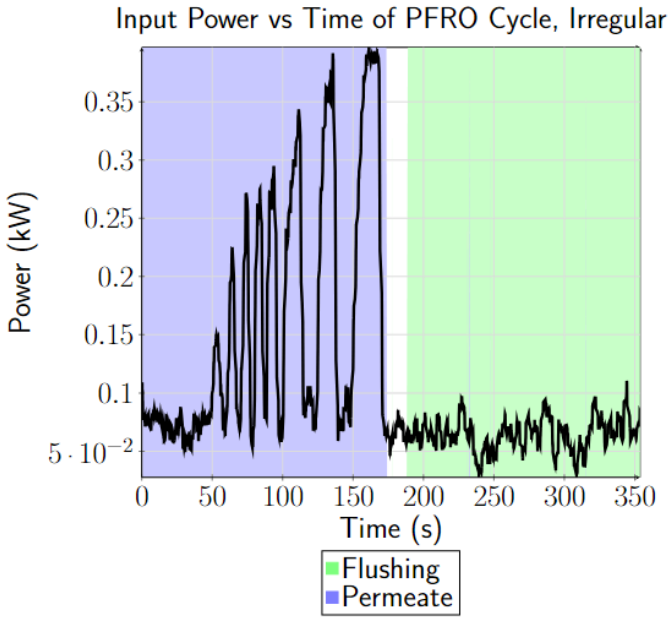

Figure 4.23: Irregular wave data of input power vs. time, with respect to PFRO cycle

Lastly, Figure 4.23 depicts input power vs time. By conducting the same analysis with the regular wave data, 41.1 kWH/m^3 of permeate produced was determined. Compared to the value of 37.1 kWh/m^3 of permeate produced by a perfectly regular, sinusoidal wave, this result makes sense as the ideal wave conditions required less energy to produce the same amount of freshwater compared to irregular wave conditions. Lastly, the recovery ratio for the irregular wave motion is calculated to be 40%. Similar SEC calculations were done with the irregular wave and the energy used was 1.03kWh/m^3.

Throughout the entire build and test process, the team ran into numerous challenges. One challenge was leak prevention. Due to the system being pressurized up to 890 psi, leaks of any kind are addressed immediately. This is due to the fact that with these high pressures, leaks can propagate and further damage the piping structure. Another issue the team faced was the motor and pump sizing. Specifically, the motor that powered the pump was too powerful for the application. Therefore, the motor was operating at its minimum rpm and it was difficult to fine tune and adjust the speed of the motor.

References

Carylsue. (2016). 4 billion people face water scarcity. Retrieved from https://blog.education.nationalgeographic.org/2016/02/15/4-billion-people-face-water-scarcity/ Encyclopedia Britannica. https://www.britannica.com/place/Puerto-Rico

Environmental Protection Agency. (2023, April). *Statistic & Facts*. EPA. https://www.epa.gov/watersense/statistics-and-facts

Gerhardt, N. (2024, March 15). *The ultimate solar panel maintenance guide to keep your panels working as efficiently as possible*. Forbes. https://www.forbes.com/home-improvement/solar/solar-panel-maintenance-tips/#:~:text=Solar%20panels%20only%20need%20maintenance,dust%20and%20debris%20can%20accumulate.

"Home." *Oneka Technologies*, 23 Jan. 2024, www.onekawater.com/.

Jason Industrial. (2023, April 10). *SAE-J1273 Hydraulic Guidelines*. https://jasonindustrial.com/guidelines/sae-j1273-hydraulic-guidelines/#:~:text=Scope%20%E2%80%93%20SAE%20J1273%20provides%20guidelines,for%20other%20hoses%20and%20systems.

KPCC, 89.3. (n.d.). San Juan Water District august water use. Retrieved from https://projects.scpr.org/applications/monthly-water-use/san-juan-water-district/

Lenntech. (n.d.). *Water treatment solutions*. Lenntech Water treatment & purification. https://www.lenntech.com/processes/electrodialysis-ed-.htm

"Marine Energy Market (by Type: Wave Energy, Tidal Energy, Ocean Thermal Energy Conversion (OTEC), Salinity Gradient Power (SGP); by Application: Power Generation, Desalination, Hydrogen Production, Other) - Global Industry Analysis, Size, Share, Growth, Trends, Regional Outlook, and Forecast 2023-2032." *Precedence Research*, www.precedenceresearch.com/marine-energy-market. Accessed 8 Feb. 2024.

Mathews, T. G. , Wagenheim, . Kal and Wagenheim, . Olga J. (2024, February 7). Puerto Rico.

Panditharatne, M. (2018, March 21). *Six months after Maria: Puerto Rico's growing health crisis*. Be a Force for the Future. https://www.nrdc.org/bio/mekela-panditharatne/six-months-after-maria-puerto-ricos-growing-health-crisis

Puerto Rico - bottled water - price, January 2024. (2024). Retrieved from https://www.globalproductprices.com/Puerto-Rico/mineral_water_prices/

Puerto Rico was promised billions for safe water. taps are still running dry. - The Washington Post. (n.d.). https://www.washingtonpost.com/nation/2022/12/08/puerto-rico-maria-fiona-water-crisis/

San Juan Water District (2024). Fees and rates. Retrieved from https://www.sjwd.org/fees-and-rates

US Department of Commerce, N. O. and A. A. (1996, November 8). NDBC station page. National Data Buoy Center. https://www.ndbc.noaa.gov/station_page.php?station=41053

United States Census Bureau (2024). American Community survey 5-year data (2009-2022). Retrieved from https://www.census.gov/data/developers/data-sets/acs-5year.html

Teams: Waves to water: Wave-powered Desalination Challenge. HeroX. (n.d.). https://www.herox.com/wavestowater/teams

3D Model of Electric actuator 177 in.lbs (20nm), 24-240V. Valworx. (n.d.). https://www.valworx.com/product/electric-actuator-221-in-lbs-24-240v-acdc

3D Models of Various 80/20 Building Components and Fittings. 80/20 Inc. (n.d.). https://8020.net/

3D Model of 3/4" Electric 3-Way Stainless T-Diverter Valve 24 VDC. Valworx. (n.d.-a). https://www.valworx.com/product/stainless-3-way-t-port-ball-valve-34-24-vdc

3D Model of Pump & Motor Assembly. Sultan Alnajdi.

Acknowledgements

Pearl JAAMS would like to thank the entire Warsinger Water Lab team for guiding and supporting us throughout our journey. Specifically, we would like to acknowledge Dr. Warsinger and Dr. Garcia for providing technical guidance beginning from the ideation phase to the final build. Additionally, the team would like to thank Ali Naderi Beni, Sultan Alanjdi, and Joel Aboderin for their expertise in the physical building process. We'd also like to acknowledge Nikitha Sam, whose presence throughout the many semester's Purdue has competed has been invaluable to the teams' continued success. Lastly, we would like to acknowledge the faculty at Herrick Labs for allowing our team to build and test within the facility.

In conclusion, our team is proud to have successfully built a device capable of desalinating water through pulse flow reverse osmosis. Without any of their help, this achievement would not have been possible.